Coordination Chemistry Reviews 254 (2010) 372–385

Contents lists available at ScienceDirect

Coordination Chemistry Reviews

journal homepage: www.elsevier.com/locate/ccr

Review

Metal ion-coupled and decoupled electron transfer

Shunichi Fukuzumi [a,b,*], Kei Ohkubo [a]

[a] Department of Material and Life Science, Graduate School of Engineering, Osaka University, SORST, Japan Science and Technology Agency, Suita, Osaka 565-0871, Japan
[b] Department of Bioinspired Science, Ewha Womans University, Seoul 120-750, Republic of Korea

Contents

ARTICLE INFO

Article history:
Received 16 June 2009
Accepted 22 October 2009
Available online 1 November 2009

Dedicated to Prof. Ralph Pearson on the occasion of his 90th birthday.

Keywords:
Electron transfer
Flavin
Benzoquinone
Fullerene
Phthalocyanine
Perylenebisimide

ABSTRACT

Effects of metal ions on thermal and photoinduced electron-transfer reactions from electron donors (D) to electron acceptors (A) are reviewed in terms of metal ion-coupled electron transfer (MCET) vs. metal ion-decoupled electron transfer (MDET). When electron transfer from D to A is coupled with binding of metal ions to $A^{\bullet-}$, such an electron transfer is defined as MCET in which metal ions accelerate the rates of electron transfer. A number of examples of electron-transfer reactions from D to A, which are energetically impossible to occur, are made possible by strong binding of metal ions to $A^{\bullet-}$ in MCET. The structures of metal ion complexes with $A^{\bullet-}$ are also discussed in relation with the MCET reactivity. The MCET reactivity of metal ions is shown to be enhanced with an increase in the Lewis acidity of metal ions. In contrast to MCET, strong binding of metal ions to $A^{\bullet-}$ results in deceleration of back electron transfer from metal ion complexes of $A^{\bullet-}$ to $D^{\bullet+}$ in the radical ion pair, which is produced by photoinduced electron transfer from D to A in the presence of metal ions, as compared with back electron transfer without metal ions. The deceleration of back electron transfer in the presence of metal ions results from no binding of metal ions to A. This type of electron transfer is defined as metal ion-decoupled electron transfer (MDET). The lifetimes of CS state ($D^{\bullet+}$–$A^{\bullet-}$) produced by photoinduced electron transfer from D to A in the D–A linked systems are also elongated by adding metal ions to the D–A systems because of the stabilization of the CS states by strong binding of metal ions to $A^{\bullet-}$ and the resulting slow MDET processes.

1. Introduction and background

Metal ions play pivotal roles in controlling biological electron-transfer processes of coenzymes such as flavins, quinones, etc. in photosynthesis and respiration [1–5]. Binding metal ions to electron acceptors (A) results in enhancement of an electron-acceptor ability of A, because the one-electron reduction potential of A is shifted to a positive direction by the stronger binding of metal ions to the radical anion ($A^{\bullet-}$) as compared to the binding to A [6–13]. According to the Nernst equation, the positive shift of E_{red} (ΔE_{red}) of A due to the complex formation with a metal ion (M^{n+}) is determined by the difference in the binding constants between M^{n+} complexes with A (K_{ox}) and $A^{\bullet-}$ (K_{red}) as given by Eq. (1) under the conditions that $K_{red}[M^{n+}] \gg 1$ [13].

$$\Delta E_{red} = \frac{RT}{F} \ln \left[\frac{K_{red}[M^{n+}]}{K_{ox}[M^{n+}] + 1} \right] \quad (1)$$

Thus, electron-transfer reactions from electron donors (D) to electron acceptors (A), which are not thermodynamically feasible to

* Corresponding author at: Department of Material and Life Science, Graduate School of Engineering, Osaka University, SORST, Japan Science and Technology Agency, Suita, 2-1 Yamada-oka, Osaka 565-0871, Japan.
E-mail address: fukuzumi@chem.eng.osaka-u.ac.jp (S. Fukuzumi).

0010-8545/$ – see front matter © 2009 Published by Elsevier B.V.
doi:10.1016/j.ccr.2009.10.020

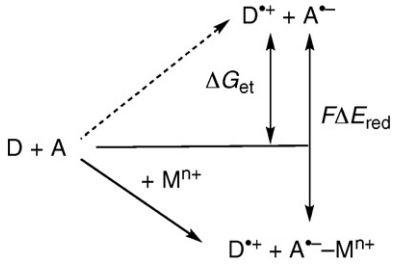

Scheme 1.

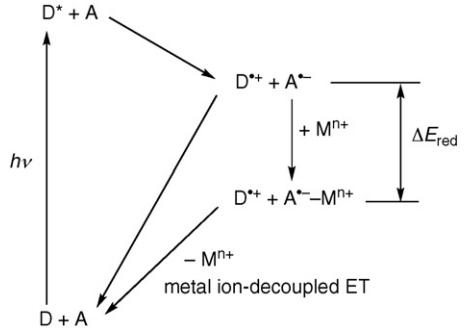

Scheme 2.

occur ($\Delta G_{et} > 0$), would occur in the presence of M^{n+} provided that the $F\Delta E_{red}$ value is larger than ΔG_{et} ($\Delta G_{et} < F\Delta E_{red}$). In such a case, the free energy change of electron transfer becomes negative ($\Delta G_{et} < 0$ in the presence of M^{n+}) as shown in Scheme 1.

Under the conditions that $K_{ox}[M^{n+}] \ll 1$, Eq. (1) is rewritten by Eq. (2). In this case, M^{n+} binds only to $A^{\bullet-}$ when virtually no

$$\Delta E_{red} = \frac{RT}{F}\ln(K_{red}[M^{n+}]) \quad (2)$$

binding of M^{n+} occurs to A. In such a case there are two reaction pathways. One is electron transfer followed by binding of M^{n+} to $A^{\bullet-}$, when electron transfer and binding of M^{n+} to $A^{\bullet-}$ occurs is a stepwise pathway. The other is a concerted pathway when electron transfer is coupled with binding of M^{n+} to $A^{\bullet-}$. The latter pathway is normally energetically more feasible because the binding of M^{n+} is coupled with electron transfer. This is defined as metal ion-coupled electron transfer (MCET) on analogy of proton-coupled electron transfer (PCET) where protonation is coupled with electron transfer [14–17].

In contrast to the case of metal ion-coupled electron transfer (MCET), the binding of M^{n+} to $A^{\bullet-}$ results in a decrease in the ET driving force of back electron transfer from $A^{\bullet-}$–M^{n+} to $D^{\bullet+}$ by ΔE_{red}, following photoinduced electron transfer from the excited state of D (D*: * denotes the excited state) to A, as shown in Scheme 2. Photoinduced electron transfer from D to A* also affords $D^{\bullet+}$ and $A^{\bullet-}$, and the driving force of back electron transfer from $A^{\bullet-}$ to $D^{\bullet+}$ becomes smaller by the binding of M^{n+} to $A^{\bullet-}$ (ΔE_{red}). Such a decrease in the ET driving force results in deceleration of the rate of back electron transfer, which is accompanied by release of M^{n+}. The electron transfer from $A^{\bullet-}$–M^{n+} to $D^{\bullet+}$ in Scheme 2 is regarded as metal ion-decoupled electron transfer (MDET) in contrast to metal ion-coupled electron transfer (MCET) in Scheme 1.

We would like to focus on contrasting effects of metal ions on MCET and MDET reactions in this review article. First a number of examples of MCET reactions are presented for both intermolecular and intramolecular ET reactions when ET rates are accelerated by binding of M^{n+} to electron acceptors and the radical anions. Then, intramolecular MDET reactions are discussed in relation with elongation of lifetimes of the charge-separated states by metal ions.

2. Intermolecular MCET

2.1. Flavins

Positive shifts of the one-electron reduction potentials of electron acceptors by binding of metal ions were first reported for flavin analogs [18]. Flavins are a ubiquitous and structurally and functionally diverse class of redox-active coenzymes that use the redox-active heteroaromatics to mediate a variety of thermal and photoinduced electron-transfer processes over a wide range of redox potentials [19–23]. Flavins are known to bind various metal ions [24–27]. For example, a flavin analog (Fl: 3-methyl-10-phenylisoalloxazine) forms complexes with metal ions such as Mg^{2+} and Zn^{2+}, Eq. (3) [18]. The formation constants K of Fl with

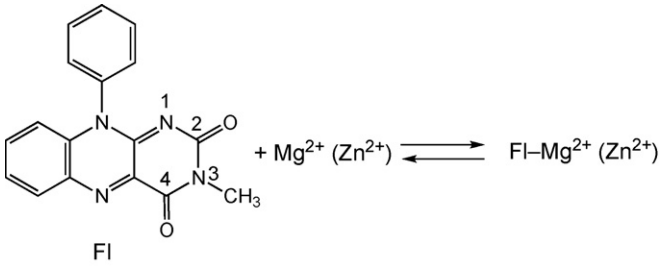

(3)

Mg^{2+} and Zn^{2+} were determined from the change in the absorption spectra by the complex formation to be 1.7×10^2 and $4.8 \times 10\,M^{-1}$, respectively [18]. Metal ions bind to the C2-carbonyl oxygen because only the C=O stretching band due to the C2-carbonyl group of Fl was significantly red-shifted by the binding of metal ions [18b]. The positive shift in the one-electron reduction potential of the singlet excited state of Fl ($^1Fl^*$) by binding of Mg^{2+} was 0.32 V [18b]. This potential shift is large enough to make photoinduced electron transfer from toluene to $^1Fl^*$ possible to occur [18b]. In the absence of Mg^{2+} no photoinduced electron transfer from toluene to $^1Fl^*$ occurs, whereas the fluorescence of $^1Fl^*$–Mg^{2+} is quenched efficiently via photoinduced electron transfer from toluene to $^1Fl^*$–Mg^{2+} (Scheme 3) [18b].

Much stronger binding of Zn^{2+} to a flavin analog than Fl in Eq. (3) has been achieved using benzodipteridine bearing a bipyridin-6-ylmethyl moiety (bpy-BDP) that acts as a metal ion binding site (Eq. (4)) [28]. The metal ion bound at the bipyridine moiety of

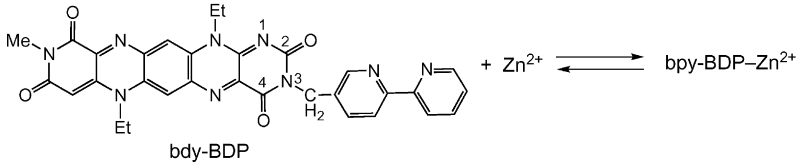

(4)

bpy-BDP is able to interact with BDP skeleton because the interaction of the metal ion bound at the bipyridine moiety with C(2)=O or C(4)=O carbonyl oxygen atoms is geometrically possible [28]. The

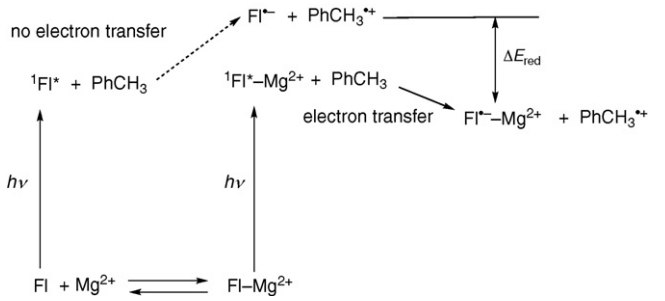

Scheme 3.

binding constant K in Eq. (4) was determined to be $3.8 \times 10^5\ M^{-1}$ [28], which is much larger than the value of Fl ($48\ M^{-1}$) in Eq. (3). In the presence of Zn^{2+}, the reduction potential of bpy-BDP was shifted in a positive direction (+0.23 V) [28]. This suggests that the oxidation activity of bpy-BDP is increased by complexation with the metal ion. In fact, the oxidizing ability of bdy-BDP was increased with Zn^{2+} by 10^3-fold for sulfite addition in methanol (MeOH) and 10^2-fold for oxidation of an NADH model compound in acetonitrile (MeCN) [28]. The oxidation active flavin model (bpy-BDP) is able to oxidize R-hydroxy acids to R-keto acids in the presence of a divalent metal ion such as Zn^{2+}, Co^{2+}, and Ni^{2+} and an amine base in MeCN [28,29].

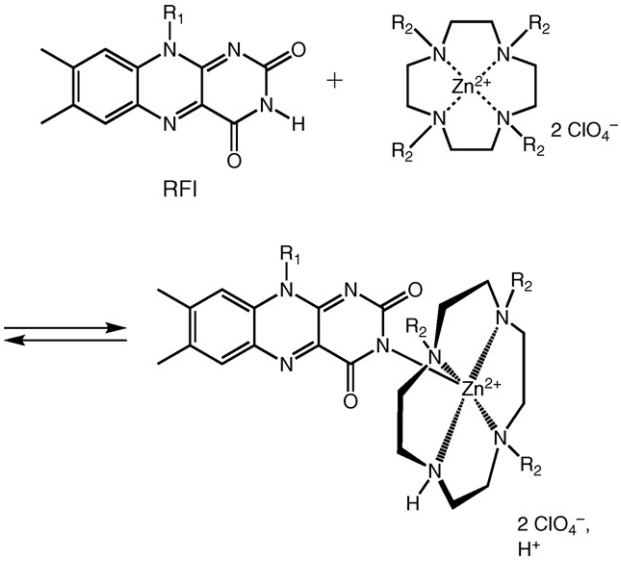

Scheme 4.

A zinc(II) tetraazacyclododecane complex (Zn(II)-cyclen) can bind to riboflavin (RFl) strongly through its deprotonated imide N^- anion in an aqueous solution (Scheme 4) [30,31]. The anion affinity constants ($\log K$) in an aqueous solution and in methanol were determined to be 5.6 [30] and 4.6 [31], respectively. The binding

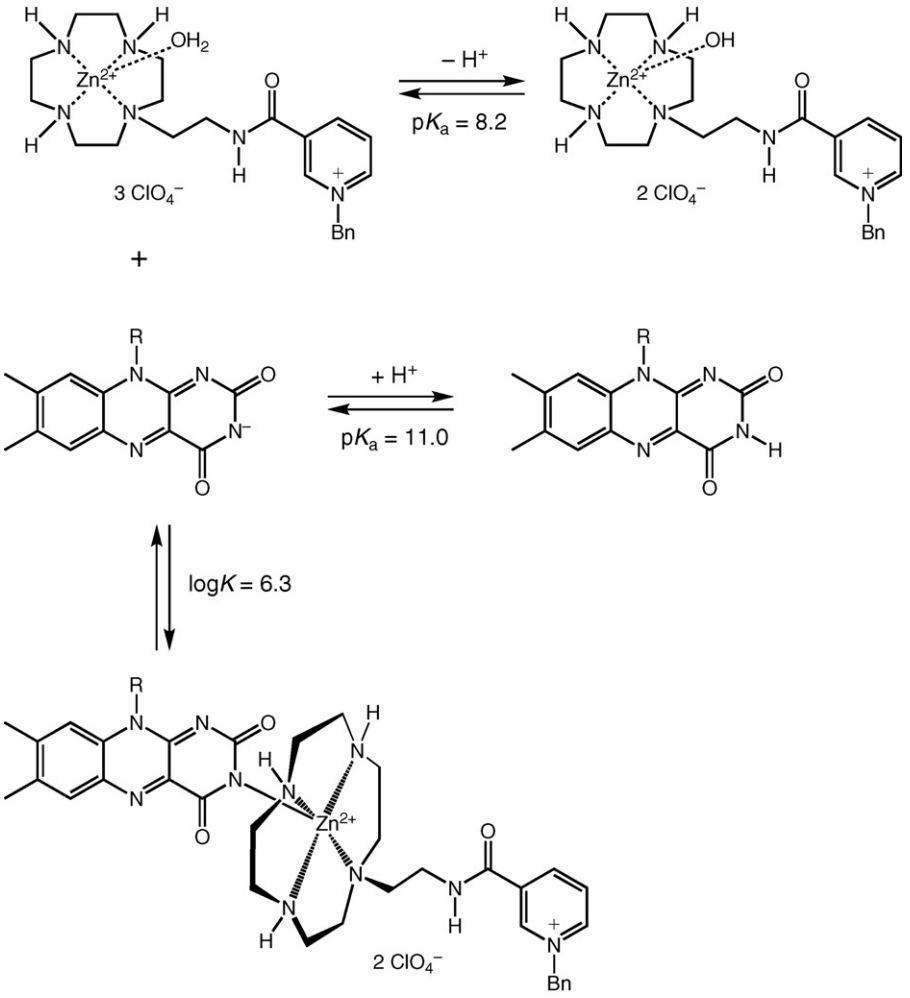

Scheme 5.

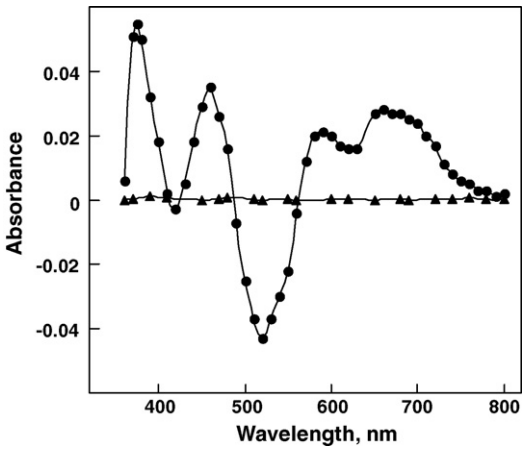

Fig. 1. Transient absorption spectra obtained by laser flash photolysis of Fl (1.0×10^{-5} M) in the absence (●) and presence of Yb^{3+} (▲, 1.0×10^{-2} M) in deaerated MeCN at 3.0 μs after laser excitation at 355 nm.

of Zn^{2+} is enhanced by hydrogen bonds between the carbonyl oxygen atoms of the imide of flavin and the NH groups of the cyclen. The binding of Zn(II)-cyclen has also a favorable influence on the reduction potentials of flavins facilitating its reduction [31].

The strong binding of Zn(II)-cyclene to RFl and enhancement of its reduction was utilized to assemble the imide-containing flavin with a suitable functionalized NADH model system to facilitate hydride transfer from an NADH model compound to RFl as shown in Scheme 5 [32]. A significant rate enhancement of up to 175 times was achieved as compared with an intermolecular reaction of an NADH model compound without the binding site for flavin [32]. In addition, a strong dependence of the reaction rate on the spacer length was observed, which clearly indicates that within the dynamic reversible assembly only the optimal relative disposition of the reactant pair ensures an efficient hydride-transfer reaction [32]. The binding of Zn^{2+} to RFl enhances both the electron-acceptor ability and the hydride-acceptor ability. There are a number of examples that hydride transfer from NADH model compounds to hydride acceptors occurs via the rate-determining electron transfer, followed by proton transfer and electron transfer [33–39]. The electron-transfer step is significantly accelerated by the binding of metal ions to hydride acceptors [40–44].

Rare-earth trivalent metal ions, which are stronger Lewis acids than Mg^{2+} and Zn^{2+} [45,46] bind strongly to a flavin analogue (riboflavin-2′,3′,4′,5′-tetraacetate, RFl) in MeCN [47]. In such a case RFl forms complexes with not only one rare-earth metal ion but also two rare-earth metal ions with binding constants K_1 and K_2, as shown in Eqs. (5) and (6), respectively [47]. The binding constants

$$\mathrm{RFl} + \mathrm{Sc^{3+}} \underset{}{\overset{K_1}{\rightleftharpoons}} \mathrm{RFl\text{-}Sc^{3+}} \quad (5)$$

$$\mathrm{RFl\text{-}Sc^{3+}} + \mathrm{Sc^{3+}} \overset{K_2}{\rightleftharpoons} \mathrm{RFl\text{-}(Sc^{3+})_2} \quad (6)$$

K_1 and K_2 for the 1:1 and 1:2 complexes of RFl with Sc^{3+} are determined as $K_1 = 3.1 \times 10^4\ M^{-1}$ and $K_2 = 1.4 \times 10^3\ M^{-1}$, respectively [47]. The complexation of RFl with rare-earth metal ions results in blue shifts of the fluorescence maximum, shortening of the fluorescence lifetime, and more importantly the change in the lowest excited state from the n,π* triplet state of RFl to the π,π* singlet states of Fl-rare-earth metal ion complexes as indicated by the disappearance of the triplet–triplet (T–T) absorption spectrum of Fl by the complexation with metal ions (Fig. 1) [47]. The non-bonding orbital is more stabilized by the complex formation with the metal ion than the π-orbital due to the stronger interaction between non-bonding electrons and the metal ion [48]. On the other hand, the π,π* singlet excited state is more stabilized by the interaction with the metal ion, that is singlet, than the π,π* triplet excited state [48]. Thus, the π,π* excited state in the Fl–metal ion complex becomes lower in energy than the n,π* singlet and triplet excited states in the uncomplexed Fl.

Table 1
Fluorescence maxima (λ_{max}), lifetimes (τ), one-electron reduction potentials (E_{red}^*) of the singlet excited states of RFl and RFl–metal ion complexes and reorganization energies of photoinduced electron transfer (λ).

Metal ion[a]	λ_{max} (nm)	τ (ns)	E_{red}^* (V) vs, SCE	λ (kcal mol^{-1})
None	506	6.5	1.67	13.6
Mg^{2+}	504	1.3	2.06	16.0
Yb^{3+}	500	0.9	2.25	18.0
Sc^{3+}	486	2.4	2.45	18.8

[a] 0.01 M.

The values of one-electron reduction potentials (E_{red}^*) of RFl–metal ion complexes at the singlet excited states are listed in Table 1 together with the fluorescence maxima (λ_{max}), fluorescence lifetimes (τ) and reorganization energies of photoinduced electron transfer (λ) [47]. The λ_{max} value is blue-shifted with increasing Lewis acidity of the metal ions. This indicates the ground state is more stabilized as compared with the excited state with increasing Lewis acidity of the metal ions. The λ values were determined by fitting the driving force dependence of the rate constant of photoinduced electron transfer from analogous series of aromatic electron donors, which have relatively small reorganization energies, to the metal ion complexes of ^{1}RFl* to the Marcus theory of electron transfer [47]. The order of E_{red}^* values (vs. SCE) is ^{1}RFl*-$(Sc^{3+})_2$ (2.45 V) > ^{1}RFl*-Yb^{3+} (2.25 V) > ^{1}RFl*-Mg^{2+} (2.06 V) > ^{1}RFl* (1.67 V), and this order is consistent with that of the formation constants (K_1) of Fl–metal ion complexes [47]. The positive shift of the E_{red}^* values with increasing Lewis acidity of the metal ions result from the large positive shift of the E_{red} values at ground state because of the binding of metal ions to $RFl^{\bullet-}$ in addition to the blue shift of the fluorescence by the metal ion binding [47].

The comparison of the E_{red}^* value of ^{1}RFl*-$(Sc^{3+})_2$ with that of ^{1}RFl* reveals the remarkable positive shifts (ca. 780 mV) of the E_{red}^* value of ^{1}RFl*-$(Sc^{3+})_2$ as compared to that of ^{1}RFl*. Such a large positive shift of the E_{red}^* value results in a significant increase in the reactivity of ^{1}RFl*-$(Sc^{3+})_2$ vs. uncomplexed RFl in the photoinduced electron-transfer reactions [47]. The larger is the positive shift of E_{red}^* with the stronger Lewis acidity of metal ions, the larger is the λ value because of the larger reorganization energy required for electron transfer that is coupled with the metal ion binding to $RFl^{\bullet-}$ (Table 1).

The binding structure of tungsten(IV) atoms to 1,3-dimethylalloxazine (DMA), which is closely related to the isoalloxazines of flavins, was revealed by the X-ray diffraction analysis as shown in Fig. 2 [49]. The tungsten(VI) atom exhibits a distorted octahedral coordination sphere and the metal is coordinated by the O4 and N5 atoms as the case of a ruthenium complex of 10-methylisoalloxazine (a flavin analog) [50,51]. The one-electron reduction of $(DMA)WO_2Cl_2$ occurs at the metal center from W^{VI} to W^{V}, whereas the one-electron reduction of $[(DMA)Cu(PPh_3)_2](BF_4)$ and $[(DMA)Ru(bpy)_2](PF_6)_2$ occurs at the DMA ligand, when the one-electron reduction potentials are positively shifted as compared to that of DMA by 0.65 and 0.86 V, respectively [49].

In contrast to a ruthenium(II) complex with 10-methylisoalloxazine [50,51], a ruthenium(II) complex of alloxazine $[Ru(Hallo)(TPA)]ClO_4$ (H_2allo = alloxazine, TPA = tris(2-pyridylmethyl)amine) forms a four-membered chelate ring with 1-N and 10-N atoms instead of a five-membered chelate ring with 4-O and 5-N, as shown in Fig. 3 [52]. The 1,10-coordination mode

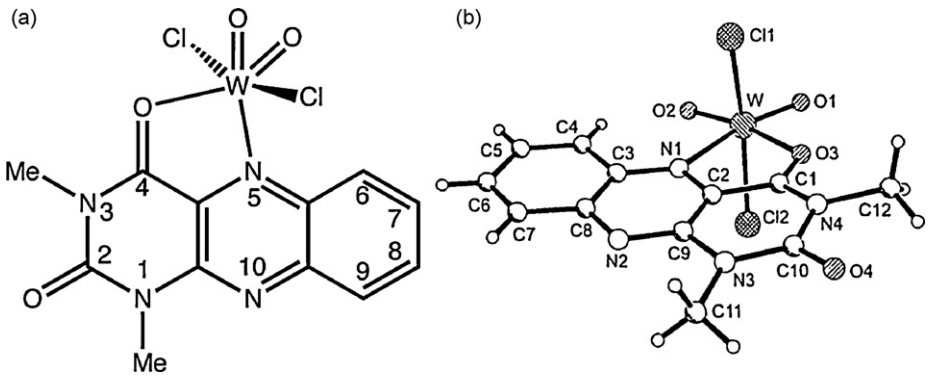

Fig. 2. (a) Molecular structure of $(DMA)WO_2Cl_2$ and (b) the X-ray crystal structure. Note the discrepancy between the superscript numbering according to heterocyclic nomenclature and the numbering from the crystal structure analysis.

in $[Ru(Hallo)(TPA)]ClO_4$ is preferred because the alloxazine ligand undergoes severe steric hindrance in 4,5-coordination in the presence of the tetradentate TPA ligand [52]. In the four-membered chelate ring of **1**, Ru-N1 distance (2.201(4) Å) is longer than Ru-N5 distance (2.116(4) Å) to reduce steric hindrance between the alloxazine ligand and the axial pyridine ring of the TPA ligand.

While the presence of metal ions that act as Lewis acids increases the reduction potential of flavins in a positive direction [18,47,53], complexation by Ru(II) lowers the reduction potential of 10-methylisoalloxazine by approximately 120 mV at neutral pH. This negative shift is caused by retrodative bonding from the metal to the ligand, which significantly increases electron density in the π system of the isoalloxazine so that it has a lower affinity for the additional electron [50,51].

2.2. Quinones

Quinones (Q) are ubiquitous in nature, playing important roles in biological energy conversion processes via electron and proton transfer [54,55]. In contrast to the case of flavins described above, *p*-benzoquinone derivatives do not form complexes with metal ions. However, the one-electron reduction potentials (E_{red}) of *p*-benzoquinone derivatives are shifted to a positive direction in the presence of metal ions due to the strong binding of metal ions to the one-electron reduced species of *p*-benzoquinone derivatives. For example, the E_{red} value of *p*-benzoquinone (Q) is shifted from −0.51 V (vs. SCE) in the absence of a metal ion to −0.01 V (vs. SCE) in the presence of $Mg(ClO_4)_2$ (1.6 M) in MeCN [56]. The positive potential shift is caused by the strong binding of Mg^{2+} to $Q^{\bullet-}$ according to Eq. (2). *p*-Benzoquinone derivatives with electron-withdrawing substituents such as 2,3-dichloro-5,6-dicyano-*p*-benzoquinone (DDQ), which has a high reduction potential (0.51 V vs. SCE), exhibit no positive potential shift in the presence of Mg^{2+} (1.6 M), because Mg^{2+} does not bind to $DDQ^{\bullet-}$. *p*-Benzoquinone derivatives with relatively low oxidation potentials ($E_{red} < -0.1$ V vs. SCE) exhibit positive potential shifts with increasing concentration of Mg^{2+} [56].

Since there are two carbonyl oxygen atoms, which can interact with Mg^{2+}, $Q^{\bullet-}$ forms not only a 1:1 complex but also a 1:2 complex with Mg^{2+}. The complex formation of $Q^{\bullet-}$ and Mg^{2+} results in the positive shift of the one-electron reduction potential of Q (E_{red}) and the Nernst equation is given by Eq. (7),

$$E_{red} = E^0_{red} + \left(\frac{2.3RT}{F}\right)\log\{K_1[M^{n+}](1 + K_2[M^{n+}])\} \quad (7)$$

where E^0_{red} is the one-electron reduction potential of Q in the absence of M^{n+}, K_1 and K_2 are the formation constants for the 1:1 and 1:2 complexes between $Q^{\bullet-}$ and Mg^{2+}, respectively [56,57].

The transient electronic spectra of the 1:1 and 1:2 complexes between semiquinone radical anions and Mg^{2+} were obtained by measuring the change in initial absorbance at various wavelengths with use of a stopped-flow spectrophotometer for electron transfer from decamethylferrocene $[Fe(Me_5C_5)_2]$ to *p*-benzoquinone derivatives in the presence of different concentrations of $Mg(ClO_4)_2$ [57,58]. The spectroscopic change in the case of the radical anion of 2,5-dichloro-*p*-benzoquinone ($Cl_2Q^{\bullet-}$) is shown in Fig. 4 [58]. Although electron transfer from $[Fe(Me_5C_5)_2]$ ($E_{ox} = -0.08$ V vs. SCE) [59] to Cl_2Q ($E_{red} = -0.18$ V vs. SCE) is endergonic ($\Delta G_{et} > 0$), the electron transfer occurs efficiently in the presence of Mg^{2+} because of the positive shift of E_{red} due to the 1:1 and 1:2 complexes between $Cl_2Q^{\bullet-}$ and Mg^{2+}. The absorption spectrum of

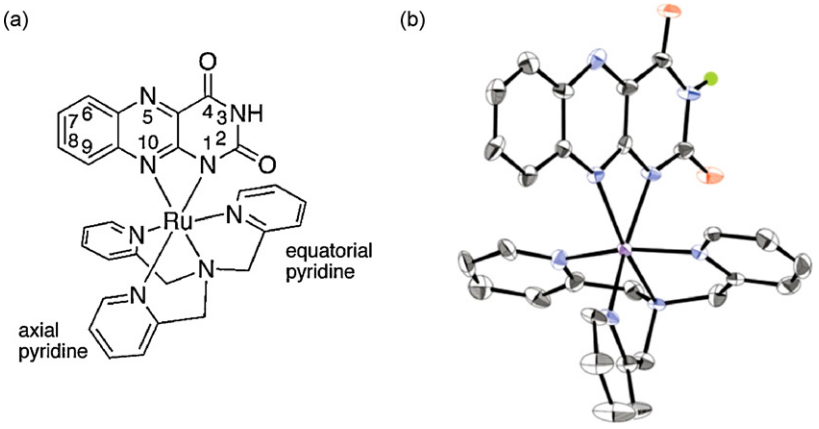

Fig. 3. (a) Molecular structure of $[Ru(Hallo)(TPA)]ClO_4$ H_2allo = alloxazine and (b) the X-ray crystal structure.

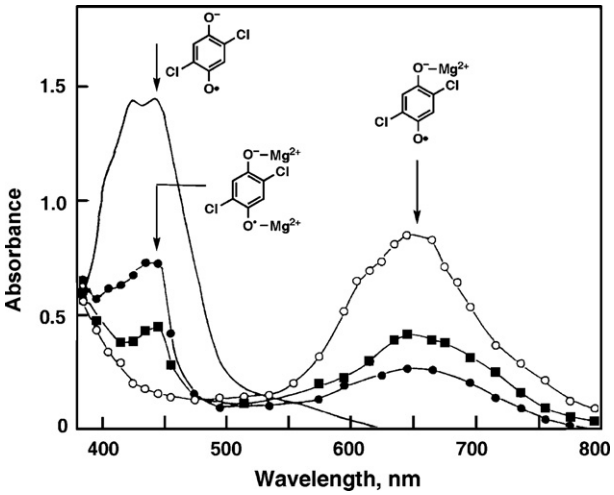

Fig. 4. Transient absorption spectra of semiquinone radical anion formed in electron-transfer reduction of 2,5-dichloro-*p*-benzoquinone (2.4×10^{-3} M) by $[Fe(Me_5C_5)_2]$ (2.4×10^{-4} M) in the presence of $Mg(ClO_4)_2$ [5.0×10^{-3} M (○), 4.0×10^{-1} M (■)] and by $[Fe(MeC_5H_4)_2]$ (2.4×10^{-4} M) in the presence of $Mg(ClO_4)_2$ [1.0 M (●)] in deaerated MeCN at 298 K. The solid line spectrum shows the absorption spectrum of semiquinone radical anion in the absence of $Mg(ClO_4)_2$, prepared by the reaction of 2,5-dichloro-*p*-benzoquinone (2.4×10^{-4} M) with $Me_4N^+OH^-$ (2.4×10^{-4} M) in deaerated MeCN at 298 K.

$Cl_2Q^{\bullet-}$ in the presence of 1.0×10^{-2} M Mg^{2+} (λ_{max} = 650 nm) is significantly red-shifted as compared to that in the absence of Mg^{2+} (λ_{max} = 450 nm) [60]. Further addition of Mg^{2+} results in a blue shift to λ_{max} = 440 nm with a clear isosbestic point. Such spectroscopic changes indicate the formation of complexes between $Cl_2Q^{\bullet-}$ and Mg^{2+}, which requires two steps; the first step is the formation of a 1:1 complex ($Cl_2Q^{\bullet-}$–Mg^{2+}) and the second step is an additional addition of Mg^{2+} to form a 1:2 complex [$Cl_2Q^{\bullet-}$–$(Mg^{2+})_2$].

The formation of Mg^{2+} complexes of semiquinone radical anions can also be confirmed by the ESR spectra [58]. An example of ESR spectra is shown in Fig. 5, where the radical anion of *p*-fluoranil ($F_4Q^{\bullet-}$) forms only the 1:1 complex with Mg^{2+} is because

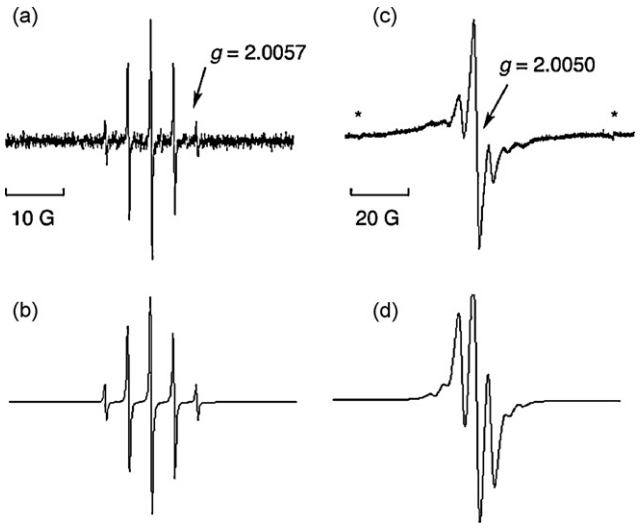

Fig. 5. (a) ESR spectrum of *p*-fluoranil radical anion formed in electron-transfer reduction of *p*-fluoranil (2.0×10^{-5} M) by $(BNA)_2$ (1.0×10^{-5} M) in deaerated MeCN at 298 K. (b) Computer simulation spectrum with g = 2.0057 with a(4F) = 3.9 G, ΔH_{msl} = 0.20 G. (c) ESR spectrum of the *p*-fluoranil radical anion–$Mg(ClO_4)_2$ complex generated in the photoirradiation of a deaerated MeCN solution of *p*-fluoranil (1.0×10^{-3} M) with $(BNA)_2$ (1.0×10^{-3} M) in the presence of $Mg(ClO_4)_2$ (1.0 M) at 298 K. Asterisk denotes Mn^{2+} marker. (d) Computer simulation spectrum with g = 2.0050 with a(2F) = 5.0 G, $a(^{25}Mg)$ = 4.1 G, ΔH_{msl} = 2.0 G.

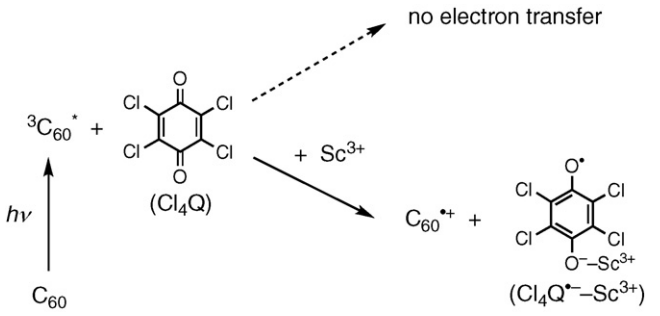

Scheme 6.

of the strong electron-withdrawing effect of fluorines [58]. First, $F_4Q^{\bullet-}$ is formed by electron transfer from dimeric 1-benzyl-1,4-dihydronicotinamide [$(BNA)_2$] to F_4Q in MeCN at 298 K, since $(BNA)_2$ acts as an electron donor to produce the radical anions of electron acceptors [61]. The ESR spectrum of $F_4Q^{\bullet-}$ is shown in Fig. 5a together with the computer simulation spectrum with the hyperfine coupling constant [*hfc*: a(4F) = 3.9 G] (Fig. 5b). Addition of $Mg(ClO_4)_2$ (1.0 M) to an MeCN solution of $F_4Q^{\bullet-}$ affords the ESR spectrum in Fig. 5c, which is well reproduced by the computer simulation spectrum with the *hfc* values including a superhyperfine coupling due to one ^{25}Mg nucleus ($a(^{25}Mg)$ = 4.1 G) which has 10.13% natural abundance as shown in Fig. 5d. The observation of such a superhyperfine coupling due to one magnesium nucleus confirms formation of the 1:1 complex between $F_4Q^{\bullet-}$ and Mg^{2+}. Due to the complexation with one Mg^{2+}, the spin is more localized on two carbons [58].

By applying electron-transfer reactions from $(BNA)_2$ to electron acceptors in the presence of metal ions, a number of metal ion complexes of radical anions of electron acceptors have been detected by ESR [62–65]. When a metal ion has a nuclear spin, the superhyperfine splitting enables to determine the number of metal ions bound to radical anions [62–65].

Among various metal ions acting as Lewis acids, Sc^{3+} has the strongest Lewis acidity because Sc^{3+} has the smallest ion radius among rare-earth trivalent metal cations [45]. The combination of *p*-benzoquinone derivatives and Sc^{3+} provides strong one-electron oxidants because of the largest positive shift of the one-electron reduction potentials [45]. For example, photoinduced electron-transfer oxidation of fullerene (C_{60}) becomes possible by using *p*-chloranil (Cl_4Q) and Sc^{3+} as shown in Scheme 6 [66]. The oxidation of C_{60} is rendered more difficult with a one-electron oxidation potential of 1.26 V vs. ferrocenium/ferrocene in comparison to the facile reduction of C_{60} [67]. Thus, no photoinduced electron transfer from $^3C_{60}{}^*$ to Cl_4Q occurs in benzonitrile (PhCN), because of the positive free energy change (ΔG_{et}) obtained from the one-electron oxidation potential of $^3C_{60}{}^*$ (E_{ox} = 0.20 V vs. SCE) and the one-electron reduction potential of *p*-chloranil (E_{red} = 0.01 V vs. SCE). In the presence of scandium triflate [$Sc(OTf)_3$] (OTf = OSO_2CF_3), however, photoexcitation with 532 nm laser light of C_{60}in PhCN containing Cl_4Q results in the appearance of a new absorption band at 980 nm which is readily assigned to $C_{60}{}^{\bullet+}$ [68–70] as shown in Fig. 6 [66]. The decay of $^3C_{60}{}^*$ at 740 nm is accompanied by the appearance of $C_{60}{}^{\bullet+}$ at 980 nm, but this species decays at prolonged reaction time (see inset of Fig. 6). The formation of the radical intermediate complex [$C_{60}{}^{\bullet+}Cl_4Q^{\bullet-}$–$Sc^{3+}$] in Scheme 6 was confirmed by the ESR spectrum observed in the Sc^{3+}-promoted photoinduced electron transfer from $^3C_{60}{}^*$ to Cl_4Q in frozen PhCN at 193 K under photoirradiation with a high-pressure mercury lamp [66]. Thus, photoinduced electron transfer from $^3C_{60}{}^*$ to Cl_4Q occurs in the presence of Sc^{3+} to produce $C_{60}{}^{\bullet+}$ and the $Cl_4Q^{\bullet-}$–Sc^{3+} complex, both of which decay via a relatively slow back electron-

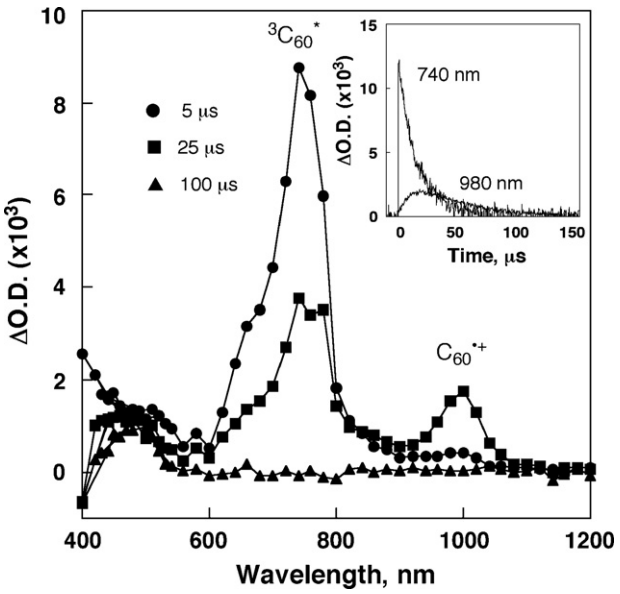

Fig. 6. Transient absorption spectra observed in photoinduced electron transfer from C_{60} (1.1×10^{-4} M) to Cl_4Q (4.0×10^{-2} M) in the presence of Sc^{3+} (0.11 M) after laser irradiation at $\lambda = 532$ nm in deaerated PhCN at 5 μs (●), 25 μs (■) and 100 μs (▲).

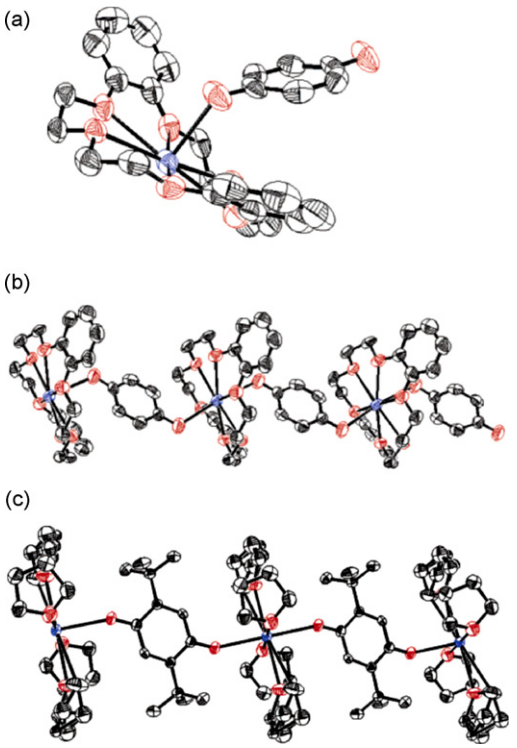

Fig. 7. (a) ORTEP diagram of the 1:1 salt K(crown ether)$^+$–Q•$^-$. (b) The interionic chain character in the crystal lattice of K(crown ether)$^+$–Q•$^-$. (c) The crystal lattice of $K(THF)_4^+$–$Bu^t_2Q^{\bullet-}$ showing the anion radical coordinated to two potassium counterions (ligated by four THF solvates) in an infinite chain.

transfer process. The strong binding between $Cl_4Q^{\bullet-}$ and Sc^{3+} makes the electron transfer energetically feasible as reported for the Sc^{3+}-catalyzed electron-transfer reduction of *p*-benzoquinone [45]. Transient absorption spectra of the radical cations of various fullerene derivatives were detected by laser flash photolysis of the fullerene/*p*-chloranil/Sc^{3+} systems [66].

The combination of a strong organic oxidant such as DDQ and $Sc(OTf)_3$ has been proven to provide a convenient and powerful oxidant for oxidative coupling reactions of oligoporphyrins [71–75] and polycyclic aromatics [76]. A bis-*N*-annulated quaterrylene, which is promising functional components in molecular devices, has been synthesized by oxidative coupling and ring fusion of easily available *N*-annulated perylene derivatives with DDQ/$Sc(OTf)_3$ (Scheme 7) [76].

2.3. Structures of metal ion complexes of semiquinone radical anions

With regard to X-ray crystal structures of metal ion complexes of semiquinone radical anions, only a few examples have so far been reported [77,78]. The binding K^+ ion to $Q^{\bullet-}$ has been clearly shown in results in 1:1 crystals of K(crown ether)$^+$–Q•$^-$ in which each K^+ ion is equatorially coordinated by crown ether and axially coordinated (via oxygen) to $Q^{\bullet-}$ as shown in Fig. 7a [77]. The opposite axial position is also occupied by an oxygen from a second $Q^{\bullet-}$ and the remaining carbonyl groups of both benzoquinones are in turn coordinated to K^+ ions, leading to the formation of the infinite anion/cation chains in Fig. 7b [77]. This type of infinite chain contact ion pairing was also observed in the crystal structure of the $K(THF)_4^+$ salt of the radical anion of 2,5-di-*tert*-butyl-*p*-benzoquinone ($Bu^t_2Q^{\bullet-}$) as shown in Fig. 7c. The close proximity of the axial oxygen atoms to K^+ with the K–O bond lengths of 2.65 and 2.73 Å is indicative of binding of K^+ to $Q^{\bullet-}$ [77]. The cation locations deviate significantly from the benzoquinone plane, the angles between the K–O and C=O bonds being 117° and 111° and the C–C–O–K torsion angles of 67° and 61° for the K^+ coordinated at opposite ends of $Q^{\bullet-}$ [77].

The dissolution of the crystal of K(crown ether)$^+$–Q•$^-$ into THF affords ESR spectra which show a significant dependence on the temperature [77]. The ESR spectrum of the THF solution of K(crown ether)$^+$–Q•$^-$ at room temperature shows the binominal quintet derived from splitting on four equivalent hydrogen atoms with a hyperfine constant of $a(4H) = 2.42$ G. However, lowering the temperature of the K(crown ether)$^+$–Q•$^-$ solution results in the selective broadening and subsequent disappearance of the hyperfine components with $M = \pm 1$, and at very low temperature the ESR spectrum shows the splitting of the two inequivalent pairs of hydrogen atoms with $a(H_\alpha) = 2.93$ and $a(H_\beta) = 1.91$ G. Such alternating line broadening and spectroscopic transformations were assigned to reversible switching of the counterion coordination from one end of $Q^{\bullet-}$ to the other as reported earlier (Eq. (8)) [78,79]. Thus, the covalent coordination of $Q^{\bullet-}$ to K^+ at one end is accom-

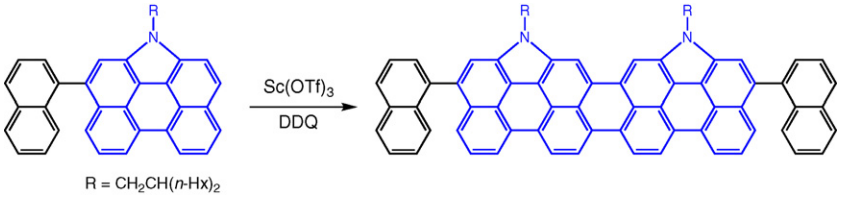

Scheme 7.

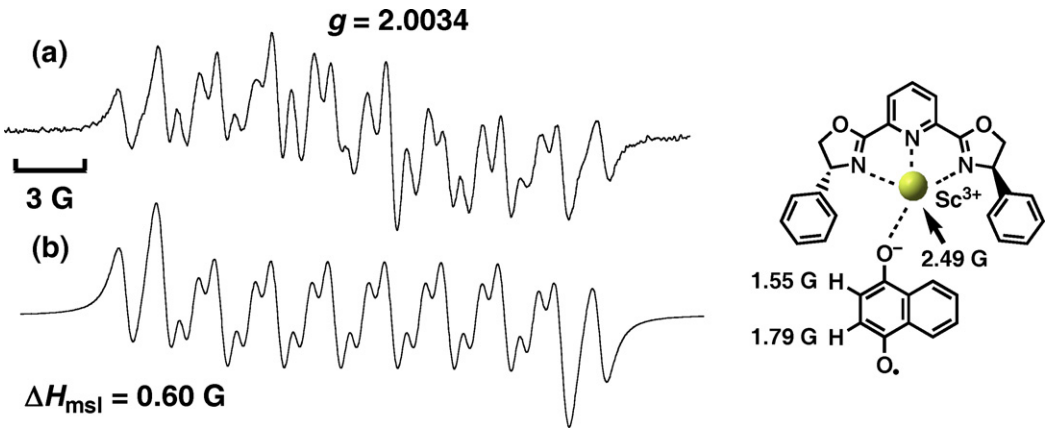

Fig. 8. ESR spectrum of a deaerated propionitrile solution of NQ (0.1 M) and NQH_2 (0.1 M) in the presence of [Sc(*R*)-pybox]$(OTf)_3$ (0.1 M) at 233 K and (d) the computer simulation spectrum.

panied by a

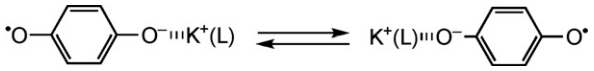

(8)

significant shift of the electron spin, and two pairs of protons become significantly inequivalent. Such a migration of K^+ from one end to the other leads to alternating line broadening. As the temperature increases, the rates of the migration become faster, such that at room temperature it is very fast on the ESR time scale, and the spectra reveal "averaged" splitting by four equivalent hydrogen atoms. From the dynamic ESR simulation the rate constant was determined to be $7 \times 10^7\ s^{-1}$ at 293 K [77]. In the case of $F_4Q^{\bullet-}$–Mg^{2+} (Fig. 5c) [58], no migration of Mg^{2+} is observed, indicating that the binding of Mg^{2+} to $F_4Q^{\bullet-}$ is stronger than that of K^+ to $Q^{\bullet-}$.

The strong binding of Sc^{3+} to semiquinone radical anions is clearly indicated by the observation of superhyperfine splitting due to the bound Sc^{3+} in an ESR spectrum of a chiral scandium complex of 2,6-bis-(oxazolinyl)pyridine, [Sc(*R*)-pybox]$(OTf)_3$ with 1,4-naphthoquinone radical anion ($NQ^{\bullet-}$) as shown in Fig. 8 [80]. The computer simulation spectrum with superhyperfine splitting due to one Sc^{3+} (a(Sc) = 2.49 G) and two inequivalent hyperfine splitting due to hydrogen atoms (a(H) = 1.55, 1.79 G) agree well with the observed ESR spectrum. The $NQ^{\bullet-}$–[Sc(*R*)-pybox]$^{3+}$ complex was produced by the comproportionation reaction between NQ and NQH_2 in the presence of [Sc(*R*)-pybox]$(OTf)_3$ [80].

The paramagnetic monomer complex, $NQ^{\bullet-}$–[Sc(*R*)-pybox]$^{3+}$ is in equilibrium with the diamagnetic chiral π-dimer metallocyclophane complexes, $(NQ^{\bullet-})_2$–([Sc(*R*)-pybox]$^{3+})_2$ [80]. The analysis of the ^{1}H NMR spectrum of $(NQ^{\bullet-})_2$–([Sc(*R*)-pybox]$^{3+})_2$ in Fig. 9a revealed the π-dimer structure in Fig. 9b (or Fig. 9c), since NOE are detected between H_B (or H_A) protons and phenyl protons of [Sc(*R*)-pybox]$^{3+}$ (termed *a*) when irradiated at H_B, supporting the calculated structure of $(NQ^{\bullet-})_2$–([Sc(*R*)-pybox]$^{3+})_2$ [80]. An enantiomer pair of the $(NQ^{\bullet-})_2$ unit in $(NQ^{\bullet-})_2$–([Sc(*R*)-pybox]$^{3+})_2$ is

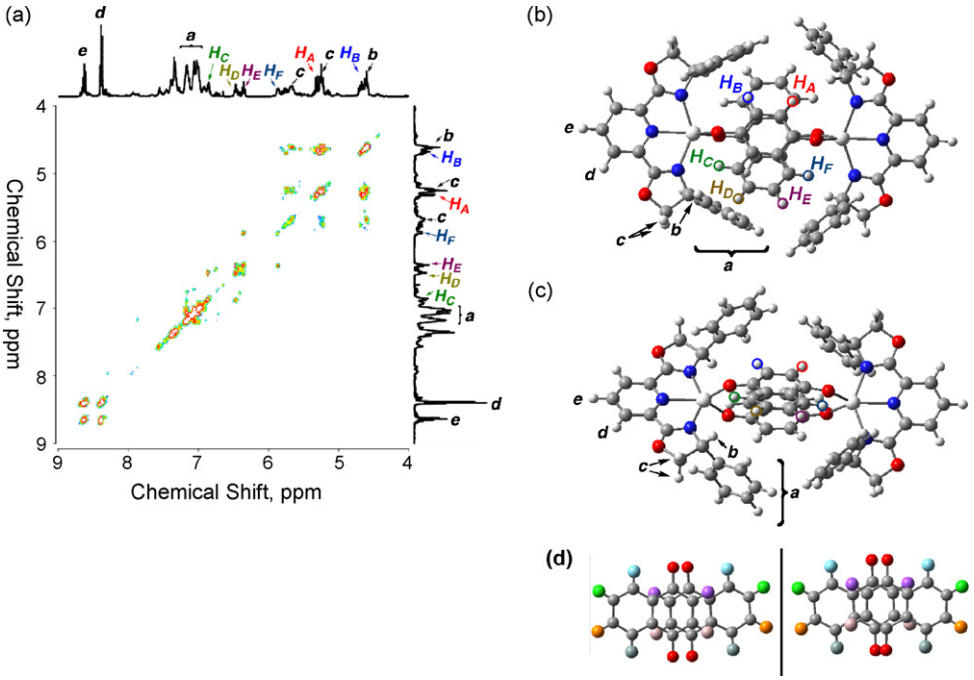

Fig. 9. (a) ^{1}H NOESY NMR spectrum of a deaerated CD_3CN solution of NQ (5.0×10^{-2} M) and Me_2Fc (5.0×10^{-2} M) in the presence of [Sc(*R*)-pybox]$(OTf)_3$ (5.0×10^{-2} M) at 298 K. The optimized structure of $(NQ^{\bullet-})_2$–([Sc(*R*)-pybox]$^{3+})_2$ calculated by using a density functional theory at the B3LYP/6-31G*: top view (b) and front view (c). (d) An enantiomer pair of the $(NQ^{\bullet-})_2$ unit in $(NQ^{\bullet-})_2$–(Sc^{3+}-pybox)$_2$.

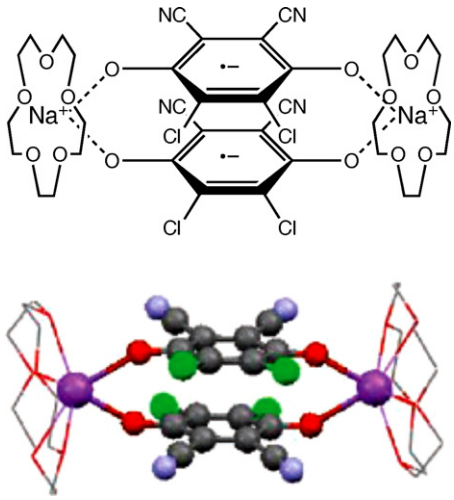

Fig. 10. Crystal structure of Na(15-crown-5)DDQ salt showing discrete dianionic dyads tethered by pairs of polyether encircled sodium counter-ions.

shown in Fig. 9d. The π–π* transition of the π-dimer complex, $(NQ^{\bullet-})_2$–$([Sc(R)\text{-pybox}]^{3+})_2$, appears at 633 nm with the Cotton effects of the CD bands with complete mirror images for their enantiomer pairs [81]. The same type of π-dimer complex was also formed for $(Q^{\bullet-})_2$–$([Sc(R)\text{-pybox}]^{3+})_2$ [81].

The π-dimer structure in the metal ion complex of the radical anion of *p*-benzoquinone derivative (Fig. 9c) was confirmed by the X-ray crystallographic analysis of $[(DDQ^{\bullet-})_2$–$Na(15\text{-crown-}5]^{+})_2$ as illustrated in Fig. 10 [81]. Within these multi-ion aggregates, benzoquinone moieties are arranged pairwise at interplanar separation of r_π = 2.86 Å, which is typical for π-dimers of $DDQ^{\bullet-}$ [82] and shifted laterally. They show elongated C=O and C=C bonds (1.247 and 1.365 Å, respectively), and shortened C–C bonds of 1.477 Å due to the radical anion character. Each $DDQ^{\bullet-}$ coordinates two Na^+ ions, with O–Na distance of d_{MO} = 2.3 and 2.5 Å, which is characteristic of contact ion pairs (CIP) [83,84]. Thus, metal ions form a bridge between π-bonded DDQ moieties to give a metallocyclophane-type complex.

3. Intramolecular MCET

Electron transfer at a fixed donor–acceptor distance plays an essential role in biological electron-transfer systems such as photosynthesis, respiration, and redox-mediated enzyme catalysis [1–5]. In this context, a number of donor–acceptor linked systems with inert rigid spacers have been developed to study the electron-transfer reactions between the donor and acceptor moieties at a fixed distance [85–89]. In each case, however, photoexcitation of the donor or acceptor moiety is required to start the electron-transfer reaction, because it would be impossible to connect donor and acceptor molecules if electron transfer occurred thermally. However, thermal intermolecular electron-transfer reactions, which would otherwise be unlikely to occur, proceed efficiently in the presence of metal ions that can promote the electron-transfer reactions (vide supra).

Intramolecular electron-transfer reactions of donor–acceptor linked molecules can also be started thermally by addition of metal ions (vide infra). A ferrocene–naphthoquinone dyad (Fc–NQ) was designed and synthesized to examine the intramolecular MCET reaction [90]. No ET from the Fc to the NQ moiety occurs in Fc–NQ thermally in MeCN at 298 K as expected from the highly positive free energy change of electron transfer (ΔG_{ET} = 1.19 eV) [90]. Addition of $Mg(OTf)_2$ to an MeCN solution of Fc–NQ still resulted in no electron transfer, whereas addition of $Sc(OTf)_3$ resulted in MCET to

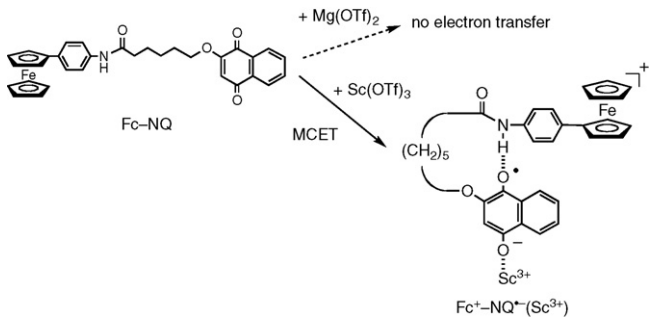

Scheme 8.

produce the Fc^+–$NQ^{\bullet-}(Sc^{3+})$ complex as indicated by appearance of the absorption band due to the Fc^+ moiety at 860 nm together with the absorption band at λ_{max} = 420 nm due to the $NQ^{\bullet-}(Sc^{3+})$ moiety (Scheme 8) [90]. Formation of Fc^+–$NQ^{\bullet-}(Sc^{3+})$ was also confirmed by the ESR spectrum [90]. According to the optimized geometry the O–H distance between the quinone oxygen atom of the $NQ^{\bullet-}$ moiety and the amide hydrogen is 1.62 Å, indicating hydrogen bond formation between them. The strong binding of Sc^{3+} to the quinone oxygen atom of the $NQ^{\bullet-}$ moiety together with the hydrogen bonding in Fc^+–$NQ^{\bullet-}$ resulted in a remarkable positive shift of the one-electron reduction potential of the NQ moiety (E_{red} vs. SCE = 1.21 V), which becomes more positive than the one-electron oxidation potential of the Fc moiety (E_{ox} vs. SCE = 0.38 V) as indicated by the cyclic voltammogram of Fc–NQ in the presence of 7.0 mM $Sc(OTf)_3$ [90]. The MCET reactions were also observed in the presence of $Y(OTf)_3$ and $Eu(OTf)_3$ [90]. The MCET reactivity agrees with the order of Lewis acidity of metal ions [45,91]. A ferrocene–quinone dyad (Fc–Q) with a rigid amide spacer also undergoes efficient MCET in the presence of various metal ions including Ba^{2+}, Ca^{2+}, Mg^{2+} as well as Sc^{3+} [92]. The MCET reactivity also agrees with the order of Lewis acidity of metal ions [92].

Intramolecular MCET reactions can be started by addition of metal ions, but they can be stopped by removal of metal ions through competitive binding of metal ions by other ligands, which results in back electron transfer to regenerate the donor–acceptor linked molecules. The back electron transfer is coupled with the removal of metal ion and such an electron-transfer process can be regarded as metal ion-decoupled electron transfer (MDET), which is discussed in more detail in the next section.

The competitive binding metal ions can be controlled by photoirradiation, because it is well known that the open form (merocyanine, MC) of spiropyran (SP) can coordinate with metal ions strongly, whereas the closed form of SP does not show the metal ion binding ability [93–95]. By taking advantage of its unique properties of SP, the intramolecular MCET processes in a TTF (tetrathiafluvalene)–quinone dyad (TTF–Q) Scheme 9 can be modulated by UV–vis light irradiation in the presence of spiropyran [96]. The addition of Pb^{2+} to a CH_2Cl_2/THF solution of TTF–Q and SP results in MCET to produce $TTF^{\bullet+}$–$Q^{\bullet-}(Pb^{2+})$ [96]. It was proposed that the synergic coordination of $Q^{\bullet-}$ and the oligoethylene glycol chain with Pb^{2+} should be responsible for stabilizing the radical ion pair state and thus facilitating the MCET process [96]. UV light irradiation of the solution resulted in a decrease in the absorbance at 845 nm due to $TTF^{\bullet+}$–$Q^{\bullet-}(Pb^{2+})$, but the subsequent visible light irradiation led to the restoration of the absorption intensity at 845 nm [96]. This is due to the release of Pb^{2+} from MC–Pb^{2+} complex after the visible light irradiation. Such decrease and increase in the absorption intensity at 845 nm can be repeated several times by applying UV light and visible light alternatively [95]. Although the MDET from $Q^{\bullet-}(Pb^{2+})$ to $TTF^{\bullet+}$ was not complete

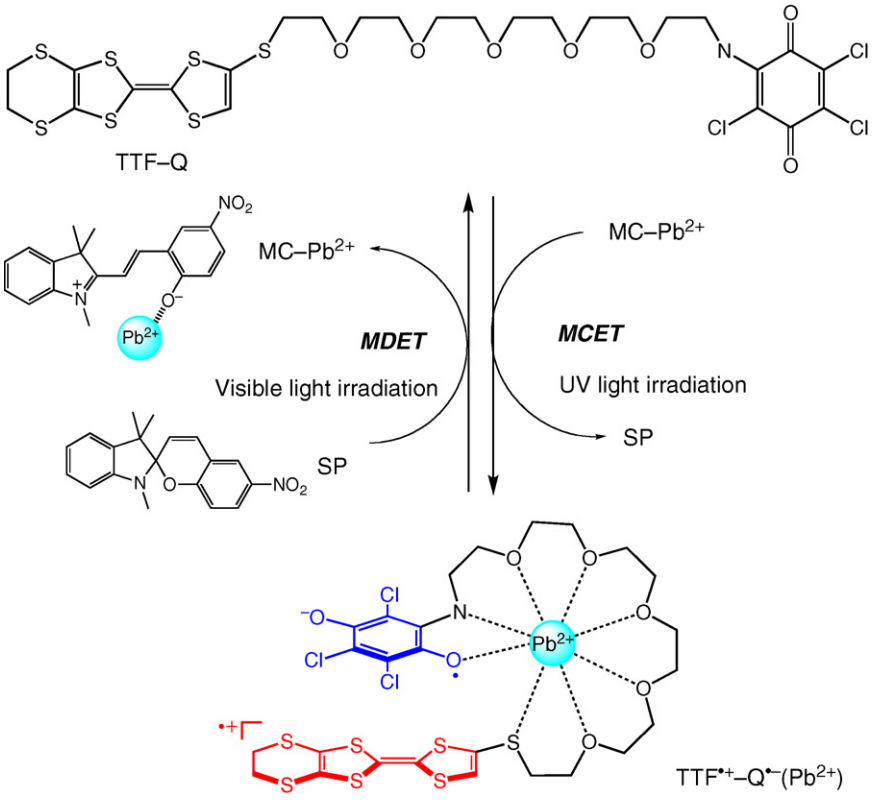

Scheme 9.

because the binding constant of MC with PC is not large enough to remove Pb^{2+} from $TTF^{\bullet+}$–$Q^{\bullet-}$(Pb^{2+}) completely, the MCET and MDET processes could be photochemically controlled by employing the unique features of SP [96]. Similar TTF–quinone dyads (TTF–Q) that contain relatively weak electron acceptors as compared with TTF–Q in Scheme 10 can also undergo MCET in the presence of metal ions [97]. A binaphthalene with two substituted TTF and trichloroquinone units also undergoes efficient MCET from the TTF units to the trichloroquinone units in the presence of a variety of metal ions (Pb^{2+}, Sc^{3+}, Zn^{2+}, and Ca^{2+}) [98].

The photochemical control of MCET and MDET processes of TTF–Q with SP in Scheme 9 has been applied to a TTF–quinone–TTF triad (TTF–Q–TTF) in which the quinone unit is substituted with the *N*,*N*-dialkylaniline unit (Scheme 10). A broad intramolecular charge transfer (ICT) band is observed at 542 nm between the quinone and *N*,*N*-dialkylaniline units in the triad, which undergoes MCET from the TTF units to the substituted quinone unit in the presence of metal ions (Pb^{2+}, Zn^{2+}, and Sc^{3+}) [99], accompanied by a decrease in the ICT intensity. The MCET and MDET processes have also been tuned by alternating UV and visible light irradi-

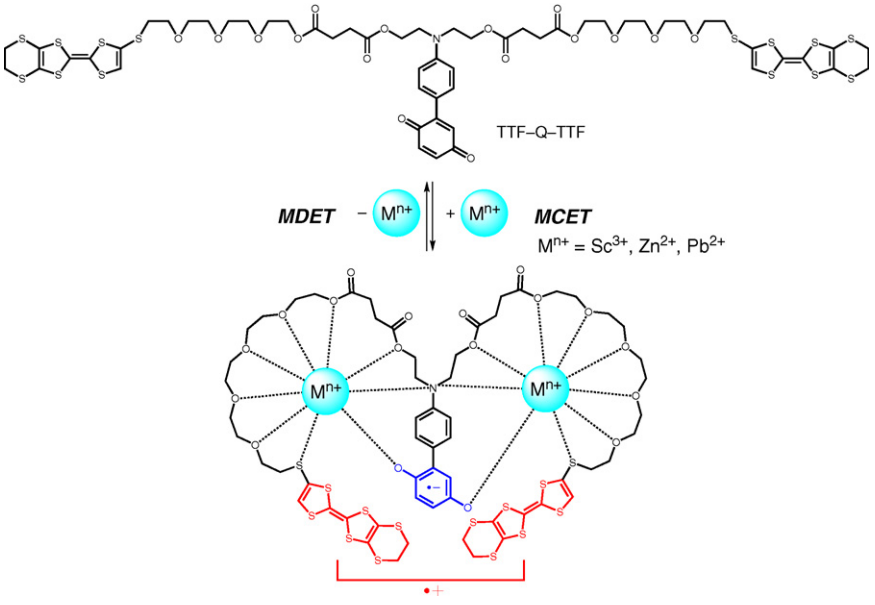

Scheme 10.

ation in the presence of SP as the case of TTF–Q in Scheme 10 [99].

4. Intramolecular metal ion-decoupled electron transfer

Binding of metal ions to radical anions of electron acceptor affects not only the thermal electron-transfer reactions but also photoinduced electron-transfer reactions, which are described in this section. The first example for the effect of metal ions on photoinduced electron transfer of electron donor–acceptor ensembles was reported for zinc porphyrin–naphthalenediimide dyad (ZnP–NIm). Laser excitation of a PhCN solution of ZnP–NIm results in efficient electron transfer from the singlet excited state of ZnP (^{1}ZnP*) to the NIm moiety to produce the charge-separated (CS) state as shown in transient absorption spectrum due to ZnP$^{\bullet+}$–NIm$^{\bullet-}$ in Fig. 11a [100]. The CS lifetime (τ_{CS}) was 1.3 μs from the first-order decay of the CS state [100]. The addition of Sc(OTf)$_3$ to a PhCN solution of ZnP–NIm results in a significant change in the transient absorption spectrum as compared to that in the absence of Sc(OTf)$_3$ as shown in Fig. 11b. At 0.1 μs, besides the absorption bands due to ZnP$^{\bullet+}$ and NIm$^{\bullet-}$, a new absorption band is observed at 650 nm, which was not seen in the absence of Sc(OTf)$_3$ in Fig. 11a. At 1 μs, the absorption bands due to NIm$^{\bullet-}$ are completely changed to those of the new bands which can be assigned to the NIm$^{\bullet-}$(Sc^{3+}) complex [100]. Although the rate of formation of the CS state was not affected by the presence of Sc^{3+}, the CS lifetime in the presence of Sc^{3+} (14 μs) was 11 times longer than that in the absence of Sc^{3+} (1.3 μs) [100]. Because Sc^{3+} does not bind to the NIm moiety of ZnP–NIm, the binding of Sc^{3+} occurs after photoinduced electron transfer from ^{1}ZnP* to NIm to produce ZnP$^{\bullet+}$–NIm$^{\bullet-}$(Sc^{3+}), when the rate of photoinduced electron transfer was not affected by the presence of Sc^{3+} [100]. Thus, electron transfer from ^{1}ZnP* to NIm and the binding of Sc^{3+} to NIm$^{\bullet-}$ occurs in a stepwise manner (not coupled). In contrast to the forward electron transfer, the back electron transfer from NIm$^{\bullet-}$(Sc^{3+}) to ZnP$^{\bullet+}$ in ZnP$^{\bullet+}$–NIm$^{\bullet-}$(Sc^{3+}) is accompanied by removal of Sc^{3+} from NIm$^{\bullet-}$ to reproduce ZnP–NIm. Such an electron-transfer process with removal of a metal ion is regarded as metal ion-decoupled electron transfer (MDET) as mentioned earlier. The elongation of the CS lifetime in the presence of Sc^{3+} results from a decrease in the driving force of back electron transfer due to the stabilization

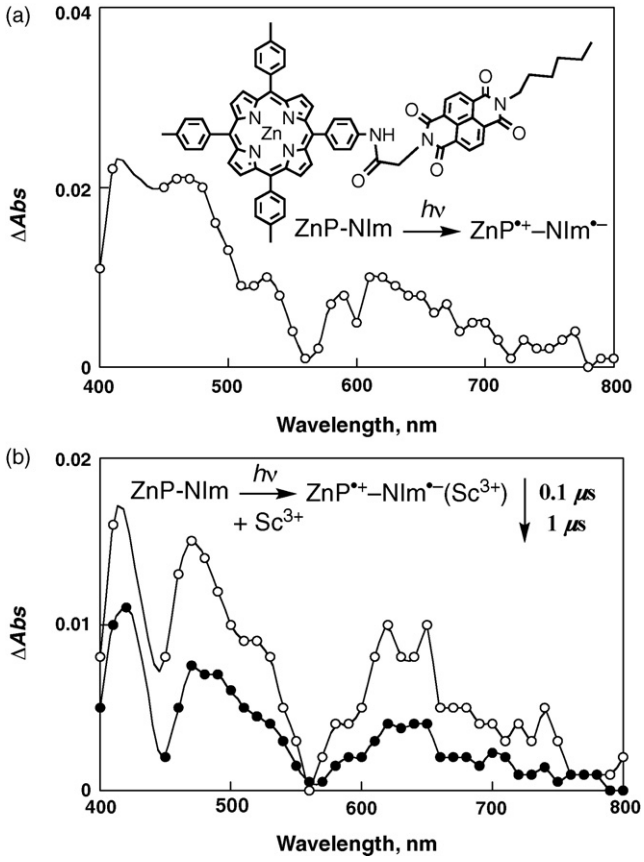

Fig. 11. (a) Time-resolved absorption spectrum observed at 0.1 μs after laser pulse excitation (431 nm) of a deaerated PhCN solution of ZnP–NIm (1.0×10^{-5} M) at 298 K. (a) Time-resolved absorption spectra of observed at 0.1 μs (○) and 1 μs (●) after laser pulse excitation (431 nm) of a deaerated PhCN solution of ZnP–NIm (1.0×10^{-5} M) in the presence of Sc(OTf)$_3$ (2.0×10^{-3} M) at 298 K.

of the CS state by binding of Sc^{3+} to NIm$^{\bullet-}$ together with an increase in the reorganization energy of MDET due to the removal of Sc^{3+} from NIm as compared with that of electron transfer in the absence of Sc^{3+} [100]. A much more remarkable increase of the CS lifetime

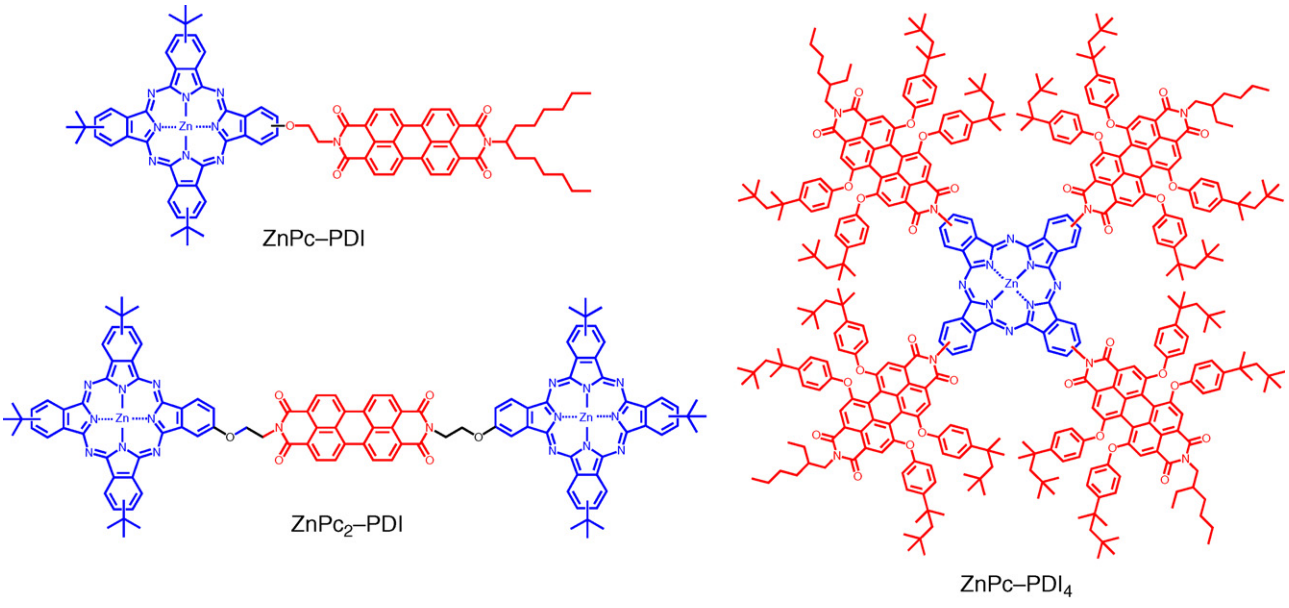

Scheme 11.

was attained for ferrocene–anthraquinone dyad (Fc–AQ) involving with a rigid amide spacer by binding of Y^{3+} to the $AQ^{\bullet-}$ moiety [101]. The CS lifetime of Fc^{+}–$AQ^{\bullet-}$ without metal ion was 12 ps, whereas that of Fc^{+}–$AQ^{\bullet-}$–(Y^{3+}) was elongated to 83 μs [101].

Long lifetimes of CS states of biomimetic electron donor–acceptor ensembles composed of multiple components mimicking the charge-separation processes in the photosynthetic reaction center have been achieved by optimizing the efficiency of the charge-separation processes between components which have small reorganization energies of electron transfer in order to accelerate the forward electron transfer in the Marcus normal region and to decelerate the back electron transfer in the Marcus inverted region [85–89,102–107]. MDET provides a totally opposite approach to attain long-lived CS states using a large reorganization energy of MDET in the Marcus normal region.

More remarkable effects of metal ions were reported for photodynamics of electron donor–acceptor ensembles containing perylenebisimides (PDIs) as compared with those containing NIm [108]. PDI act as electron acceptors, are widely used as chromophores as electron transporting materials in technological devices since these molecules have outstanding stability and strong absorption bands in the visible region [109,110]. On the other hand, phthalocyanines (Pcs) have magnificent absorption in the 600–700 nm region, leading to a blue-coloring ability, which is accompanied by a robust nature, acting as electron donors [111]. Thus, combination of Pcs and PDIs dyes provides excellent light harvesting properties [112–115]. However, photoexcitation of a zinc phthalocyanine–perylenediimide dyad (ZnPc–PDI), a bis(zinc phthalocyanine)–perylenediimide triad [$(ZnPc)_2$–PDI], and a zinc phthalocyanine–perylenebisimide pentad [ZnPc–$(PDI)_4$] (Scheme 11) results in formation of the triplet excited state of the PDI moiety without the fluorescence emission because of the low lying triplet excited state of PDI (1.07 eV), which is lower in energy than the CS state (1.25 eV) [108].

The addition of Mg^{2+} ions to PhCN solutions of ZnPc–PDI, $(ZnPc)_2$–PDI, and ZnPc–$(PDI)_4$ results in formation of long-lived CS states, $ZnPc^{\bullet+}$–$PDI^{\bullet-}$–(Mg^{2+}): τ_{CS} = 240 μs, and $(ZnPc)_2{}^{\bullet+}$–$PDI^{\bullet-}$–$(Mg^{2+})^{+}$: τ_{CS} = 270 μs, and $ZnPc^{\bullet+}$–$PDI^{\bullet-}$–(Mg^{2+})$(PDI)_3$: τ_{CS} = 480 μs, respectively [108]. The energy diagram is shown in Scheme 12, where the energy of

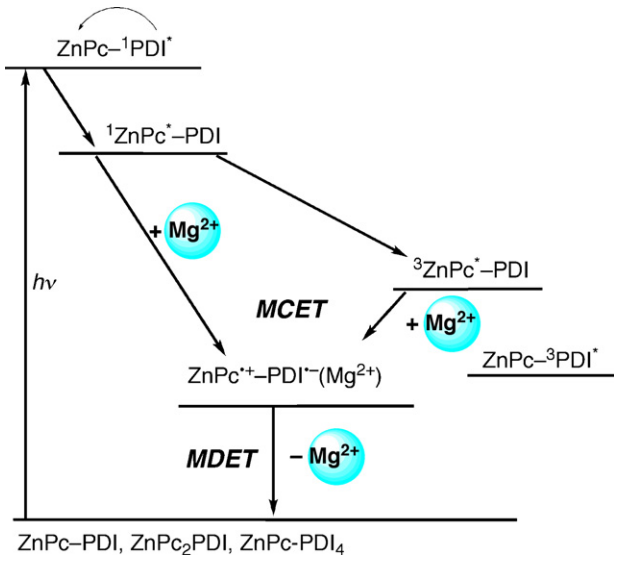

Scheme 12.

the CS state in the presence of 0.10 M Mg^{2+} (0.79 eV) is lower than the triplet excited state of the PDI moiety (1.07 eV). The long CS lifetimes result from the strong binding of Mg^{2+} with the $PDI^{\bullet-}$ moiety, which decelerate the MDET process for charge recombination to the ground state.

The slowest MDET rate of CS state of an electron donor–acceptor dyad with metal ion has been reported as shown in Scheme 13 [116]. In the absence of metal ion, no electron transfer from the singlet excited state of C_{60} ($^1C_{60}$*) to the trinitrofluorenone (TNF) moiety in the dyad was observed in PhCN by nanosecond laser flash photolysis, since the energy of CS state ($C_{60}{}^{\bullet+}$–$TNF^{\bullet-}$: 1.89 eV) is higher than that of $^1C_{60}$* (1.75 eV). As the case of intermolecular photoinduced electron transfer from C_{60} to Cl_4Q with Sc^{3+} described earlier [66], C_{60} can be oxidized by intramolecular electron transfer with aromatic carbonyl compounds with Sc^{3+}. The addition of $Sc(OTf)_3$ (30 mM) to a PhCN solution containing C_{60}–TNF results in drastic change in the photodynamics from the formation

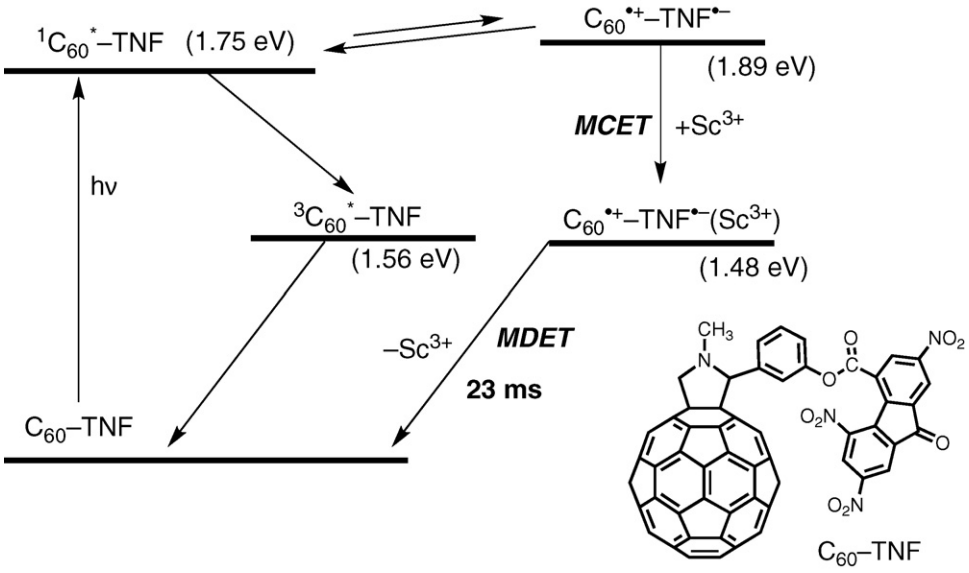

Scheme 13.

of $^3C_{60}$* to electron transfer to produce the CS state in which Sc^{3+} binds to $TNF^{\bullet-}$ [$TNF^{\bullet-}(Sc^{3+})$]. The energy of CS state is decreased by binding of Sc^{3+} to the $TNF^{\bullet-}$ moiety of the CS state (1.48 eV). The CS lifetime of $C_{60}{}^{\bullet+}$–$TNF^{\bullet-}(Sc^{3+})$ was determined to be 23 ms in PhCN at 298 K, which is the longest lifetime ever reported for electron donor–acceptor linked systems in solution [116].

5. Summary

Since metal ions act as Lewis acids and radical anions of electron acceptors ($A^{\bullet-}$) are bases, metal ions bind much more strongly to $A^{\bullet-}$ as compared to A. The large difference in the binding constants of metal ions with $A^{\bullet-}$ and A results in a large positive shift of the one-electron reduction potentials of A (E_{red}) according to Eq. (1). Such a large positive shift of A due to the strong binding of metal ions to $A^{\bullet-}$ makes a drastic change in the energetics of electron transfer from D to A. A number of examples have been demonstrated for both thermal and photoinduced electron-transfer reactions from D to A, which were impossible to occur without metal ions, are made possible by simply adding metal ions to the D–A systems. In such cases, electron transfer is coupled with binding metal ions to $A^{\bullet-}$ and this type of electron transfer is defined as metal ion-coupled electron transfer (MCET). The MCET reactivity of metal ions increases with an increase in the Lewis acidity of metal ions.

When electron transfer from D to A is energetically feasible without metal ions particularly in exergonic photoinduced electron-transfer reactions, electron transfer and binding of metal ions to $A^{\bullet-}$ occurs in a stepwise manner, i.e., metal ions bind to $A^{\bullet-}$ after the electron transfer. The back electron transfer from metal ion complexes with $A^{\bullet-}$ to $D^{\bullet-}$, which are produced by photoinduced electron transfer, involves removal of metal ions from $A^{\bullet-}$ when metal ions do not bind to A. This type of electron transfer is defined as metal ion-decoupled electron transfer (MDET). The lifetimes of CS state ($D^{\bullet+}$–$A^{\bullet-}$) produced by photoinduced electron transfer from D to A in the D–A linked systems can be elongated by adding metal ions to the D–A systems because of the stabilization of the CS states by strong binding of metal ions to $A^{\bullet-}$ and the slow MDET processes. The scope and applications of MCET and MDET processes are expected to expand further in the near future.

Acknowledgements

The author gratefully acknowledges the contributions of their collaborators and coworkers mentioned in the references. The authors acknowledge continuous support of their study by Grants-in-Aid from the Ministry of Education, Culture, Sports, Science and Technology, Japan and KOSEF/MEST through WCU project (R31-2008-000-10010-0) in Korea.

References

[1] W. Kaim, B. Schwederski, Bioinorganic Chemistry: Inorganic Elements in the Chemistry of Life, John Wiley & Son, Chichester, 1994.
[2] A.J. Hoff, J. Deisenhofer, Phys. Rep. 287 (1997) 2.
[3] J. Deisenhofer, J.R. Norris (Eds.), The Photosynthetic Reaction Center, Academic Press, San Diego, 1993.
[4] S. Ferguson-Miller, G.T. Babcock, Chem. Rev. 96 (1996) 2889.
[5] C.F. Yocum, Coord. Chem. Rev. 252 (2008) 296.
[6] S. Fukuzumi, in: V. Balzani (Ed.), Electron Transfer in Chemistry, vol. 4, Wiley–VCH, Weinheim, 2001, p. 3.
[7] S. Fukuzumi, Bull. Chem. Soc. Jpn. 70 (1997) 1.
[8] S. Fukuzumi, S. Itoh, in: D.C. Neckers, D.H. Volman, G. von Bünau (Eds.), Advances in Photochemistry, vol. 25, Wiley, New York, 1998, p. 107.
[9] S. Fukuzumi, S. Itoh, Antioxid. Redox Signal. 3 (2001) 807.
[10] S. Fukuzumi, Org. Biomol. Chem. 1 (2003) 609.
[11] S. Fukuzumi, Bull. Chem. Soc. Jpn. 79 (2006) 177.
[12] S. Fukuzumi, Prog. Inorg. Chem. 56 (2009) 49.
[13] R.A. Marcus, H. Eyring, Annu. Rev. Phys. Chem. 15 (1964) 155.
[14] R.I. Cukier, D.G. Nocera, Annu. Rev. Phys. Chem. 49 (1998) 337.
[15] C.J. Chang, M.C.Y. Chang, N.H. Damrauer, D.G. Nocera, Biochim. Biophys. Acta 1655 (2004) 13.
[16] J.M. Mayer, I.J. Rhile, Biochim. Biophys. Acta 1655 (2004) 51.
[17] M.H.V. Huynh, T.J. Meyer, Chem. Rev. 107 (2007) 5004.
[18] (a) S. Fukuzumi, S. Kuroda, T. Tanaka, Chem. Lett. (1984) 417; (b) S. Fukuzumi, S. Kuroda, T. Tanaka, J. Am. Chem. Soc. 107 (1985) 3020.
[19] (a) C.T. Walsh, Acc. Chem. Res. 13 (1980) 148; (b) C.T. Walsh, Acc. Chem. Res. 19 (1986) 216.
[20] T.C. Bruice, Acc. Chem. Res. 13 (1980) 256.
[21] P.F. Heelis, R.F. Hartman, S.D. Rose, Chem. Soc. Rev. (1995) 289.
[22] S. Fukuzumi, T. Tanaka, in: M.A. Fox, M. Chanon (Eds.), Photoinduced Electron Transfer, Part C, Elsevier, Amsterdam, 1988, p. 636.
[23] G. Tollin, in: V. Balzani (Ed.), Electron Transfer in Chemistry, vol. 4, Wiley–VCH, Weinheim, 2001, p. 202.
[24] J. Lauterwein, P. Hemmerich, J.-M. Lhoste, Inorg. Chem. 14 (1975) 2152.
[25] (a) M.J. Clarke, Comments Inorg. Chem. 3 (1984) 133; (b) M.J. Clarke, Rev. Inorg. Chem. 2 (1980) 27.
[26] W. Kaim, B. Schwederski, O. Heilmann, F.M. Hornung, Coord. Chem. Rev. 182 (1999) 323.
[27] S. Fukuzumi, T. Kojima, J. Biol. Inorg. Chem. 13 (2008) 321.
[28] H. Ohshiro, K. Mitsui, N. Ando, Y. Ohsawa, W. Koinuma, H. Takahashi, S. Kondo, T. Nabeshima, Y. Yano, J. Am. Chem. Soc. 123 (2001) 2478.
[29] (a) Y. Yano, K. Mitsui, Y. Ohsawa, T. Kobayashi, T. Nabeshima, J. Chem. Soc. Chem. Commun. (1993) 1719; (b) N. Ando, Y. Ohsawa, T. Nabeshima, Y. Yano, Chem. Lett. (1996) 381.
[30] M. Shinoya, E. Kimura, M. Shiro, J. Am. Chem. Soc. 115 (1993) 6730.
[31] B. König, M. Pelka, R. Reichenbach-Klinke, J. Schelter, J. Daub, Eur. J. Org. Chem. (2001) 2297.
[32] R. Reichenbach-Klinke, M. Kruppa, B. König, J. Am. Chem. Soc. 124 (2002) 12999.
[33] (a) S. Fukuzumi, T. Tanaka, Chem. Lett. (1982) 1513; (b) S. Fukuzumi, K. Hironaka, T. Tanaka, Chem. Lett. (1982) 1583; (c) S. Fukuzumi, K. Hironaka, T. Tanaka, J. Am. Chem. Soc. 105 (1983) 4722; (d) S. Fukuzumi, N. Nishizawa, T. Tanaka, J. Org. Chem. 49 (1984) 3571.
[34] (a) S. Fukuzumi, Y. Kondo, T. Tanaka, Chem. Lett. (1983) 751; (b) S. Fukuzumi, Y. Kondo, T. Tanaka, J. Chem. Soc. Perkin Trans. 2 (1984) 673.
[35] S. Fukuzumi, S. Koumitsu, K. Hironaka, T. Tanaka, J. Am. Chem. Soc. 109 (1987) 305.
[36] P. Van Eikeren, P. Kenney, R. Tokmakian, J. Am. Chem. Soc. 101 (1979) 7402.
[37] S. Fukuzumi, K. Ohkubo, Y. Tokuda, T. Suenobu, J. Am. Chem. Soc. 122 (2000) 4286.
[38] A. Anne, J. Moiroux, J.M. Saveant, J. Am. Chem. Soc. 115 (1993) 10224.
[39] X.Q. Zhu, Y. Yang, M. Zhang, J.P. Cheng, J. Am. Chem. Soc. 125 (2003) 15298.
[40] R.A. Gase, U.K. Pandit, J. Am. Chem. Soc. 101 (1979) 7059.
[41] S. Fukuzumi, Y. Fujii, T. Suenobu, J. Am. Chem. Soc. 123 (2001) 10191.
[42] S. Fukuzumi, J. Yuasa, T. Suenobu, J. Am. Chem. Soc. 124 (2002) 12566.
[43] J. Yuasa, S. Yamada, S. Fukuzumi, J. Am. Chem. Soc. 128 (2006) 14938.
[44] S. Fukuzumi, H. Kotani, Y.M. Lee, W. Nam, J. Am. Chem. Soc. 130 (2008) 15134.
[45] (a) S. Fukuzumi, K. Ohkubo, Chem. Eur. J. 6 (2000) 4532; (b) K. Ohkubo, T. Suenobu, H. Imahori, A. Orita, J. Otera, S. Fukuzumi, Chem. Lett. (2001) 978.
[46] (a) S. Fukuzumi, K. Ohkubo, J. Am. Chem. Soc. 124 (2002) 10270; (b) K. Ohkubo, S.C. Menon, A. Orita, J. Otera, S. Fukuzumi, J. Org. Chem. 68 (2003) 4720.
[47] S. Fukuzumi, K. Yasui, T. Suenobu, K. Ohkubo, M. Fujitsuka, O. Ito, J. Phys. Chem. A 105 (2001) 10501.
[48] S. Fukuzumi, N. Satoh, T. Okamoto, K. Yasui, T. Suenobu, Y. Seko, M. Fujitsuka, O. Ito, J. Am. Chem. Soc. 123 (2001) 7756.
[49] F.M. Hornung, O. Heilmann, W. Kaim, S. Zalis, J. Fiedler, Inorg. Chem. 39 (2000) 4052.
[50] M.J. Clarke, M.G. Dowling, A.R. Garafalo, T.F. Brennan, J. Biol. Chem. 255 (1980) 3472.
[51] M.J. Clarke, M.G. Dowling, A.R. Garafalo, T.F. Brennan, J. Am. Chem. Soc. 255 (1983) 223.
[52] S. Miyazaki, T. Kojima, K. Ohkubo, S. Fukuzumi, Angew. Chem. Int. Ed. 46 (2007) 905.
[53] M.M. Morrison, D.T. Sawyer, J. Am. Chem. Soc. 100 (1978) 211.
[54] R.E. Blankenship, Molecular Mechanism of Photosynthesis, Blackwell Science, Cambridge, MA, 2001.
[55] B.L. Trumpower (Ed.), Function of Quinones in Energy-Conserving Systems, Academic Press, New York, 1986.
[56] S. Fukuzumi, N. Nishizawa, T. Tanaka, J. Chem. Soc. Perkin Trans. 2 (1985) 371.
[57] S. Fukuzumi, T. Okamoto, J. Am. Chem. Soc. 115 (1993) 11600.
[58] S. Fukuzumi, K. Ohkubo, T. Okamoto, J. Am. Chem. Soc. 124 (2002) 14147.
[59] S. Fukuzumi, S. Mochizuki, T. Tanaka, Inorg. Chem. 28 (1989) 2459.
[60] S. Fukuzumi, T. Yorisue, Bull. Chem. Soc. Jpn. 65 (1992) 715.
[61] (a) M. Patz, Y. Kuwahara, T. Suenobu, S. Fukuzumi, Chem. Lett. (1997) 567; (b) S. Fukuzumi, T. Suenobu, M. Patz, T. Hirasaka, S. Itoh, M. Fujitsuka, O. Ito, J. Am. Chem. Soc. 120 (1998) 8060.
[62] (a) J. Yuasa, T. Suenobu, S. Fukuzumi, J. Am. Chem. Soc. 125 (2003) 12090; (b) J. Yuasa, S. Fukuzumi, Org. Biomol. Chem. 2 (2004) 642.
[63] S. Fukuzumi, N. Satoh, J. Yuasa, K. Ohkubo, J. Am. Chem. Soc. 126 (2004) 7585.
[64] J. Yuasa, T. Suenobu, S. Fukuzumi, ChemPhysChem 7 (2006) 942.
[65] J. Yuasa, T. Suenobu, S. Fukuzumi, J. Phys. Chem. A 109 (2005) 9356.
[66] S. Fukuzumi, H. Mori, H. Imahori, T. Suenobu, Y. Araki, O. Ito, K.M. Kadish, J. Am. Chem. Soc. 123 (2001) 12458.

[67] Q. Xie, F. Arias, L. Echegoyen, J. Am. Chem. Soc. 115 (1993) 9818.
[68] C.A. Reed, R.D. Bolskar, Chem. Rev. 100 (2000) 1075.
[69] C.A. Reed, K.C. Kim, R.D. Bolskar, L.J. Mueller, Science 289 (2000) 101.
[70] S. Fukuzumi, K. Ohkubo, H. Imahori, D.M. Guldi, Chem. Eur. J. 9 (2003) 1585.
[71] A. Tsuda, A. Osuka, Science 293 (2001) 79.
[72] M. Kamo, A. Tsuda, Y. Nakamura, N. Aratani, K. Furukawa, T. Kato, A. Osuka, Org. Lett. 5 (2003) 2079.
[73] (a) A. Tsuda, Y. Nakamura, A. Osuka, Chem. Commun. (2003) 1096;
(b) T. Ikeue, N. Aratani, A. Osuka, Isr. J. Chem. 45 (2005) 293.
[74] S. Hiroto, A. Osuka, J. Org. Chem. 70 (2005) 4054.
[75] N.K.S. Davis, M. Pawlicki, H.L. Anderson, Org. Lett. 10 (2008) 3945.
[76] Y. Li, Z. Wang, Org. Lett. 11 (2009) 1385.
[77] J.M. Lü, S.V. Rosokha, I.S. Neretin, J.K. Kochi, J. Am. Chem. Soc. 128 (2006) 16708.
[78] K.S. Chen, N. Hirota, J. Phys. Chem. 82 (1978) 1133.
[79] S. Kabaya, Z. Luz, D. Goldfarb, J. Am. Chem. Soc. 116 (1994) 5805.
[80] J. Yuasa, S. Fukuzumi, J. Am. Chem. Soc. 129 (2007) 12912.
[81] S.V. Rosokha, J. Lu, T.Y. Rosokha, J.K. Kochi, Phys. Chem. Chem. Phys. 11 (2009) 324.
[82] J.-M. Lu, S.V. Rosokha, J.K. Kochi, J. Am. Chem. Soc. 125 (2003) 12161.
[83] J.-M. Lu, S.V. Rosokha, I.S. Neretin, J.K. Kochi, J. Am. Chem. Soc. 128 (2006) 16708.
[84] J.-M. Lu, S.V. Rosokha, S.V. Lindeman, I.M. Neretin, J.K. Kochi, J. Am. Chem. Soc. 127 (2005) 1797.
[85] (a) M.R. Wasielewski, Chem. Rev. 92 (1992) 435;
(b) K.D. Jordan, M.N. Paddon-Row, Chem. Rev. 92 (1992) 395;
(c) J.W. Verhoeven, Adv. Chem. Phys. 106 (1999) 603.
[86] (a) D. Gust, T.A. Moore, A.L. Moore, in: V. Balzani (Ed.), Electron Transfer in Chemistry, vol. 3, Wiley–VCH, Weinheim, 2001, p. 272;
(b) D. Gust, T.A. Moore, A.L. Moore, Acc. Chem. Res. 34 (2001) 40.
[87] (a) S. Fukuzumi, D.M. Guldi, in: V. Balzani (Ed.), Electron Transfer in Chemistry, vol. 2, Wiley–VCH, Weinheim, 2001, p. 270;
(b) D.M. Guldi, Chem. Commun. (2000) 321.
[88] (a) D.M. Guldi, M. Prato, Acc. Chem. Res. 33 (2000) 695;
(b) D.M. Guldi, Chem. Soc. Rev. 31 (2002) 22.
[89] (a) S. Fukuzumi, Phys. Chem. Chem. Phys. 10 (2008) 2283;
(b) S. Fukuzumi, T. Kojima, J. Mater. Chem. 18 (2008) 1427.
[90] S. Fukuzumi, K. Okamoto, H. Imahori, Angew. Chem. Int. Ed. 41 (2002) 620.
[91] K. Okamoto, H. Imahori, S. Fukuzumi, J. Am. Chem. Soc. 125 (2003) 7014.
[92] (a) S. Fukuzumi, Y. Yoshida, K. Okamoto, H. Imahori, Y. Araki, O. Ito, J. Am. Chem. Soc. 124 (2002) 6794;
(b) S. Fukuzumi, K. Okamoto, Y. Yoshida, H. Imahori, Y. Araki, O. Ito, J. Am. Chem. Soc. 125 (2003) 1007.
[93] J.D. Winkler, C.M. Bowen, V.J. Michelet, J. Am. Chem. Soc. 120 (1998) 3237.
[94] G. Wang, A.K. Bohaty, I. Zharov, H.S. White, J. Am. Chem. Soc. 128 (2006) 13553.
[95] G.Y. Wen, J. Yan, Y.C. Zhou, D.Q. Zhang, L.Q. Mao, D.B. Zhu, Chem. Commun. (2006) 3016.
[96] H. Wu, D. Zhang, L. Su, K. Ohkubo, C. Zhang, S. Yin, L. Mao, Z. Shuai, S. Fukuzumi, D. Zhu, J. Am. Chem. Soc. 129 (2007) 6839.
[97] H. Wu, D. Zhang, D. Zhu, Tetrahedron Lett. 48 (2007) 8951.
[98] H. Wu, D. Zhang, G. Zhang, D. Zhu, J. Org. Chem. 73 (2008) 4271.
[99] Y. Zeng, G. Zhang, D. Zhang, D. Zhu, J. Org. Chem. 74 (2009) 4375.
[100] K. Okamoto, Y. Mori, H. Yamada, H. Imahori, S. Fukuzumi, Chem. Eur. J. 10 (2004) 474.
[101] (a) H. Imahori, K. Tamaki, D.M. Guldi, C. Luo, M. Fujitsuka, O. Ito, Y. Sakata, S. Fukuzumi, J. Am. Chem. Soc. 123 (2001) 2607;
(b) H. Imahori, D.M. Guldi, K. Tamaki, Y. Yoshida, C. Luo, Y. Sakata, S. Fukuzumi, J. Am. Chem. Soc. 123 (2001) 6617;
(c) H. Imahori, Y. Sekiguchi, Y. Kashiwagi, T. Sato, Y. Araki, O. Ito, H. Yamada, S. Fukuzumi, Chem. Eur. J. 10 (2004) 3184.
[102] D.M. Guldi, H. Imahori, K. Tamaki, Y. Kashiwagi, H. Yamada, Y. Sakata, S. Fukuzumi, J. Phys. Chem. A 108 (2004) 541.
[103] (a) S. Fukuzumi, K. Ohkubo, H. Imahori, J. Shao, Z. Ou, G. Zheng, Y. Chen, R.K. Pandey, M. Fujitsuka, O. Ito, K.M. Kadish, J. Am. Chem. Soc. 123 (2001) 10676;
(b) K. Ohkubo, H. Kotani, J. Shao, Z. Ou, K.M. Kadish, Y. Chen, G. Zheng, R.K. Pandey, M. Fujitsuka, O. Ito, H. Imahori, S. Fukuzumi, Angew. Chem. Int. Ed. 43 (2004) 853;
(c) K. Ohkubo, H. Imahori, J. Shao, Z. Ou, K.M. Kadish, Y. Chen, R.K. Pandey, M. Fujitsuka, O. Ito, S. Fukuzumi, J. Phys. Chem. A 106 (2002) 10991.
[104] (a) S. Fukuzumi, H. Kotani, K. Ohkubo, S. Ogo, N.V. Tkachenko, H. Lemmetyinen, J. Am. Chem. Soc. 126 (2004) 1600;
(b) H. Kotani, K. Ohkubo, S. Fukuzumi, J. Am. Chem. Soc. 126 (2004) 15999;
(c) K. Ohkubo, H. Kotani, S. Fukuzumi, Chem. Commun. (2005) 4520;
(d) S. Fukuzumi, H. Kotani, K. Ohkubo, Phys. Chem. Chem. Phys. 10 (2008) 5159.
[105] (a) K. Ohkubo, S. Fukuzumi, Bull. Chem. Soc. Jpn. 82 (2009) 303;
(b) K. Ohkubo, S. Fukuzumi, J. Porphyrins Phthalocyanines 12 (2008) 993.
[106] (a) K. Okamoto, Y. Araki, O. Ito, S. Fukuzumi, J. Am. Chem. Soc. 126 (2004) 56;
(b) K. Ohkubo, R. Garcia, P.J. Sintic, T. Khoury, M.J. Crossley, K.M. Kadish, S. Fukuzumi, Chem. Eur. J. 15 (2009) 10493.
[107] F. D'Souza, R. Chitta, K. Ohkubo, M. Taisor, N.K. Subbaiyan, M.E. Zandler, M.K. Rogacki, D.T. Gryko, S. Fukuzumi, J. Am. Chem. Soc. 130 (2008) 14263.
[108] (a) S. Fukuzumi, K. Ohkubo, J. Ortiz, A.M. Gutiérrez, F. Fernández-Lázaro, Á. Sastre-Santos, Chem. Commun. (2005) 3814;
(b) S. Fukuzumi, K. Ohkubo, J. Ortiz, A.M. Gutiérrez, F. Fernández-Lázaro, Á. Sastre-Santos, J. Phys. Chem. A 112 (2008) 10744;
(c) F.J. Céspedes-Guirao, K. Ohkubo, S. Fukuzumi, Á. Sastre-Santos, F. Fernández-Lázaro, J. Org. Chem. (2009) 5871.
[109] F. Würthner, Chem. Commun. (2004) 1564.
[110] M.R. Wasielewski, J. Org. Chem. 71 (2006) 5051.
[111] C.C. Leznoff, A.B.P. Lever (Eds.), Phthalocyanines: Properties and Applications, vol. 1–4, VCH, Weinheim, 1989, 1993, 1996.
[112] X. Li, L.E. Sinks, B. Rybtchinski, M.R. Wasielewski, J. Am. Chem. Soc. 126 (2004) 10810.
[113] (a) M.S. Rodríguez-Morgade, T. Torres, C. Atienza-Castellanos, D.M. Guldi, J. Am. Chem. Soc. 128 (2006) 15145;
(b) A.J. Jiménez, F. Spänig, M.S. Rodríguez-Morgade, K. Ohkubo, S. Fukuzumi, D.M. Guldi, T. Torres, Org. Lett. 9 (2007) 2481.
[114] R.F. Kelley, W.S. Shin, B. Rybtchinski, L.E. Sinks, M.R. Wasielewski, J. Am. Chem. Soc. 129 (2007) 3173.
[115] (a) F. D'Souza, R. Chitta, S. Gadde, L.M. Rogers, P.A. Karr, M.E. Zandler, A.S.D. Sandanayaka, Y. Araki, O. Ito, Chem. Eur. J. 13 (2007) 916;
(b) F. D'Souza, E. Mailigaspe, K. Ohkubo, M.E. Zandler, N.K. Subbaiyan, S. Fukuzumi, J. Am. Chem. Soc. 131 (2009) 8787.
[116] K. Ohkubo, J. Ortiz, L. Martín-Gomis, F. Fernández-Lázaro, Á. Sastre-Santos, S. Fukuzumi, Chem. Commun. (2007) 589.